Historic, archived document

Do not assume content reflects current scientific knowledge, policies, or practices

Reserve
A290
So322

Portland Branch Library
U. S. Dept. of Agriculture

UNITED STATES DEPARTMENT OF AGRICULTURE
Soil Conservation Service
Washington, D. C.

PRELIMINARY STUDIES ON THE DEVELOPMENT OF A BAFFLE-TYPE ENERGY DISSIPATOR FOR PIPE OUTLETS.

The Two-Dimensional Investigation

by

Brooks T. Morris
Assoc. Hydraulic Engr.

James T. Rostron
Jr. Hydraulic Engr.

U. S. Soil Conservation Service,
Office of Research
Cooperative Laboratory
California Institute of Technology,
Pasadena, California

Region 10
Pacific Southwest Region
Office of Reg'l Engineering
Berkeley, California

May 1942

LIBRARY
RECEIVED
MAR 26 1954
U. S. DEPT. OF AGRICULTURE

Portland

UNITED STATES
DEPARTMENT OF AGRICULTURE
LIBRARY

Reserve
BOOK NUMBER A290
869308 So322

869308

UNITED STATES DEPARTMENT OF AGRICULTURE
Soil Conservation Service
Washington, D. C.
H. H. Bennett, Chief

PRELIMINARY STUDIES ON THE DEVELOPMENT OF A BAFFLE-TYPE ENERGY DISSIPATOR FOR PIPE OUTLETS

The Two-Dimensional Investigation

by

Brooks T. Morris
Assoc. Hydraulic Engr.
Sedimentation Division
Office of Research

James T. Rostron
Jr. Hydraulic Engr.
Southern California Area
Pacific Southwest Region

Soil Conservation Service

Office of Research
Cooperative Laboratory
California Institute of Technology
Pasadena, California

Region 10
Pacific Southwest Region
Office of Regional Engineering
Berkeley, California

May 1942

UNITED STATES DEPARTMENT OF AGRICULTURE
Soil Conservation Service
Washington, D. C.
H. H. Bennett, Chief

PRELIMINARY STUDIES ON THE DEVELOPMENT

OF A

BAFFLE-TYPE MEMORY DISSIPATOR FOR PIPE OUTLETS

The Two-Dimensional Investigation

by

Brooks T. Morris
Assoc. Hydraulic Engr.

James T. Pearson
Jr. Hydraulic Engr.

Sedimentation Division
Office of Research

Southern California Area
Pacific Southwest Region

Soil Conservation Service

Office of Research
Cooperative Laboratory
California Institute of Technology
Pasadena, California

Region 10
Pacific Southwest Region
Office of Regional Engineering
Berkeley, California

May 1942

TABLE OF CONTENTS

		Page
I	INTRODUCTION	1 - 4
II	TWO-DIMENSIONAL STUDIES	
	A. Straight Biff-Walls	5 - 24
	B. Capped Biff-Walls.	25 - 43
	C. Capped Biff-Walls with Dropped Floors	44 - 47
III	SUMMARY	48
IV	APPENDIX	49 - 50

TABLE OF CONTENTS

Page

I INTRODUCTION . . . . . 1 - 4

II TWO-DIMENSIONAL STUDIES

A. Straight Butt-Welds . . . . . 5 - 24

B. Capped Butt-Welds. . . . . 25 - 43

C. Capped Butt-Welds with

Dropped Floors . . . . . 44 - 47

III SUMMARY 48

IV APPENDIX . . . . . 49 - 50

DEVELOPMENT OF A BAFFLE-TYPE ENERGY-DISSIPATOR FOR PIPE OUTLETS

Brooks T. Morris and James T. Rostron

1942

LABORATORY STUDIES

Satisfactory design criteria for energy dissipators for pipe outlets have been available only for hydraulic jump designs. The relatively high cost of the long structures required to spread water from a pipe outlet and conduct it through the hydraulic jump has justified a search for shorter, less expensive designs in which baffles and "stilling pools" might be used to establish some other energy-dissipating flow-pattern at lower cost.

Baffle and spreader devices have been constructed by other organizations for use at the downstream ends of conduits through earth dams. These devices have been developed by means of laboratory experiment but sufficient study has not been given to any one design to permit its general use without confirmatory laboratory tests. Since such tests would be prohibitive in cost if charged to individual structures as built by the Soil Conservation Service, it is necessary to carry each laboratory study through to the point where results capable of general application are obtained.

For the development of an economical design for a baffle-type energy-dissipator for pipe outlets a general laboratory study has been undertaken. In the interest of keeping the period of the laboratory study down to a minimum time, as well as for the purpose of maintaining simplicity in field construction, experiments have been confined to the simplest, most elementary structures capable of dissipating energy. Each element added to the design, however beneficial it may be, adds a variable to the list of experimental unknowns. In the present state of the science of hydraulics, such additions all too often require the multiplication of the number of laboratory runs by 5. Obviously, then,

DEVELOPMENT OF A BAFFLE-TYPE
ENERGY-DISSIPATOR FOR PIPE OUTLETS

Brooks T. Morris and James T. Pearson

1962

LABORATORY STUDIES

Satisfactory design criteria for energy dissipators for pipe outlets have been available only for hydraulic jump design. The relatively high cost of the long structures required to spread water from a pipe outlet and conduct it through the hydraulic jump has justified a search for shorter, less expensive designs in which baffles and "stilling pools" might be used to establish some other energy-dissipating flow-pattern at lower cost.

Baffle and spreader devices have been constructed by other organizations for use at the downstream ends of conduits through earth dams. These devices have been developed by means of laboratory experiment but sufficient study has not been given to any one design to permit its general use without confirmatory laboratory tests. Since such tests would be prohibitive in cost if charged to *individual* structures as built by the Soil Conservation Service, it is necessary to carry each laboratory study through to the point where results capable of General application are obtained.

For the development of an economical design for a baffle-type energy-dissipator for pipe outlets a general laboratory study has been undertaken. In the interest of keeping the period of the laboratory study down to a minimum time, as well as for the purpose of maintaining simplicity in field construction, experiments have been confined to the simplest, most elementary structures capable of dissipating energy. Each element added to the design, however beneficial it may be, adds a variable to the list of experimental unknowns. In the present state of the science of hydraulics, such additions all too often require the multiplication of the number of laboratory runs by 5. Obviously, then,

simple structures may be studied in experiments of 25 to 125 runs while the more complex devices might require 625 or 3125. Two methods that go hand in hand can, sometimes, shorten the path from the recognition of the problem to the proof of the answer. The first is analysis, based on the few basic principles so far established in hydraulics. The second is the use of simplified models in which limited extensions of these basic principles to the analysis of a particular problem may be checked.

A single basic principle on which energy-dissipator designs may be developed is that described by Rouse in Sec. 70 of Chapter XIII of Fluid Mechanics for Hydraulic Engineers, Engineering Societies Monograph Series, McGraw-Hill N.Y. 1938. Stated more simply and in terms of our problem, this principle would be:

The energy converted to turbulence in a given stream reach is proportional to the initial kinetic energy of the flow. In this proportion, the coefficient of proportionality is determined by the geometrical pattern of the flow. In flow around pipe elbows at high Reynolds Numbers, this geometrical pattern remains the same over a wide range of velocities. The principle then is demonstrated by the constancy of the coefficient of head loss at the bend.

In open-channel energy-dissipators of all but the most minute size the geometrical pattern of flow is assumed to be determined by the fixed outlines of the dissipator walls and conduits and by a Froude Number of flow through the structure. This Froude Number may be written $F = \frac{V^2}{gd}$, wherein:

V = the mean velocity of flow
g = the acceleration of gravity
d = a length term, usually a depth

To determine experimentally the energy dissipation possibilities of a given series of structural elements, such as a pipe outlet, a box and a biff-wall, it is necessary to vary the geometric proportions of those elements and to vary the Froude Number of the flow.

simple structures may be studied in experiments of 25 to 125 runs while the more complex devices might require 625 or 3125. Two methods that go hand in hand can, sometimes, shorten the path from the recognition of the problem to the proof of the answer. The first is analysis, based on the few basic principles so far established in hydraulics. The second is the use of simplified models in which limited extensions of these basic principles to the analysis of a particular problem may be checked.

A single basic principle on which energy-dissipator design may be developed is that described by Bowes in Sec. 70 of Chapter XIII of Fluid Mechanics for Hydraulic Engineers, Engineering Societies Monograph Series, McGraw-Hill N.Y. 1938. Stated more simply and in terms of our problem, this principle would be:

The energy converted to turbulence in a given stream reach is proportional to the initial kinetic energy of the flow. In this proportion, the coefficient of proportionality is determined by the geometrical pattern of the flow. In flow around pipe elbows at high Reynolds Numbers, this geometrical pattern remains the same over a wide range of velocities. The principle then is demonstrated by the constancy of the coefficient of head loss at the bend.

In open-channel energy-dissipators of all but the most minute size the geometrical pattern of flow is assumed to be determined by the fixed outlines of the dissipator walls and controls and by a Froude Number of flow through the structure. This Froude Number may be written $F = \frac{q}{\sqrt{gs}}$, wherein:

q = a length term, usually a depth
g = the acceleration of gravity
A = the mean velocity of flow

To determine experimentally the energy dissipation possibilities of a given series of structural elements, such as a pipe outlet, a pool and a pile-wall, it is necessary to vary the geometric proportions of those elements and to vary the Froude Number of the flow.

In most energy dissipators several regimes of flow are possible, depending on the proportions of the device and the Froude Number of the flow. Within each regime of flow the variation of the coefficient of energy loss is systematic. The first purpose of a series of laboratory tests is to determine the critical proportions and Froude Numbers bounding the different regimes. Often as in open-channel flow, it is necessary only to determine the critical values of the Froude Number. More laboratory study (or analysis) is necessary, if, as in the hydraulic jump itself, the working range involves a significant and continuous variation of the coefficient of loss with the Froude Number.

Within each regime of flow, the geometrical proportions, i.e., the shape of the energy-dissipating chamber, control the amount of energy dissipation. This amount is not easily predicted. The best of the analyses, all based on the momentum equation, have been accepted only when compared with carefully conducted experiments. (For instance, the hydraulic jump equation of Belanger awaited acceptance for decades.) The momentum analysis most directly applicable to the baffle outlet problem is that developed for the study of the diffusion of jets.

Experiments for the development of baffle-type energy dissipators for pipe outlets have been designed so as to identify various regimes of flow for various heights, shapes and location of biff-wall and for various pipe-width to box-width ratios and to determine the critical proportions and Froude Numbers (or quantities of flow) between which these regimes are stable. The preliminary report has to do with the most promising flow patterns and the proportions of structure through which they are obtained.

Values of the loss coefficient, i.e. the percent energy loss, have been obtained by approximate methods and have been used in selecting the flow regimes of most use.

(Two additional criteria, aside from maximum energy dissipation and minimum cost of structure, enter into the selection of the best hydraulic design from a series of laboratory model tests. The first is stabil-

In most energy dissipators several regimes of flow are possible, depending on the proportions of the device and the Froude Number of the flow. Within each regime of flow the variation of the coefficient of energy loss is systematic. The first purpose of a series of laboratory tests is to determine the critical proportions and Froude Numbers bounding the different regimes. Often as in open-channel flow, it is necessary only to determine the critical values of the Froude Number. More laboratory study (or analysis) is necessary, if, as in the hydraulic jump itself, the working range involves a significant and continuous variation of the coefficient of loss with the Froude Number.

Within each regime of flow, the geometrical proportions, i.e., the shape of the energy-dissipating chamber, control the amount of energy dissipation. This amount is not easily predicted. The best of the analyses, all based on the momentum equation, have been accepted only when compared with carefully conducted experiments. (For instance, the hydraulic jump equation of Belanger received acceptance for decades.) The momentum analysis most directly applicable to the bottle outlet problem is that developed for the study of the dilution of jets.

Experiments for the development of bottle-type energy dissipators for pipe outlets have been designed so as to identify various regimes of flow for various heights, shapes and location of *bill-well* and for various *pipe-width to box-width* ratios and to determine the critical proportions and Froude Numbers (or quantities of flow) between which these regimes are stable. The preliminary report has to do with the most promising flow patterns and the proportions of structure through which they are obtained.

Values of the loss coefficient, i.e. the percent energy loss, have been obtained by approximate methods and have been used in selecting the flow regimes of most use.

(Two additional criteria, aside from maximum energy dissipation and minimum cost of structure, enter into the selection of the best hydraulic design from a series of laboratory model tests. The first is stabil-

ity of the flow pattern. The second is the minimization of air entrainment. If a flow pattern temporarily established by given boundary outlines and a given Froude Number can either shift to another more stable pattern or oscillate from one outline to another, the dangers of securing only insufficient energy dissipation or of developing large shock forces are considered too great for the design to be acceptable. Only is exhaustive tests should prove the safety of a pendulating flow design would it ever be used in practice.)

(The matter of air entrainment is not so easily disposed of. It is possible for bulking or buoyancy, produced by mixing of air into the water, to render unstable an otherwise satisfactory flow pattern. Neither satisfactory methods for analysing air entrainment effects nor satisfactory methods for producing them on a small scale in the laboratory have as yet been developed. All that can be done is to differentiate between various designs as to air entrainment opportunity and resistance to buoyancy effects and to observe structures both in the laboratory and in the field. Model laws for air entrainment remain to be derived.)

Recalling the vast number of runs required for simultaneous experiments on all the variable dimensions and design features at once, we have simplified the initial tests to an extreme degree.

ity of the flow pattern. The second is the minimization of air entrain-
ment. If a flow pattern temporarily established by given boundary out-
lines and a given Froude Number can either shift to another more stable
pattern or oscillate from one outline to another, the dangers of accum-
ting only insufficient energy dissipation or of developing large shock
forces are considered too great for the design to be acceptable. Only
is exhaustive tests should prove the safety of a pendulating flow de-
sign would it ever be used in practice.)

(The matter of air entrainment is not so easily disposed of. It is
possible for pulling or buoyancy, produced by mixing of air into the
water, to render unstable an otherwise satisfactory flow pattern.
Neither satisfactory methods for analyzing air entrainment effects nor
satisfactory methods for producing them on a small scale in the labora-
tory have as yet been developed. All that can be done is to differen-
tiate between various designs as to air entrainment opportunity and
resistance to buoyancy effects and to observe structures both in the
laboratory and in the field. Model laws for air entrainment remain to
be derived.)

Recalling the vast number of runs required for simultaneous experi-
ments on all the variable dimensions and design features at once, we
have simplified the initial tests to an extreme degree.

TWO-DIMENSIONAL STUDIES

Straight Biff-Walls (Without Caps)

First, a two-dimensional model was constructed in which the lateral expansion from pipe to baffle box was temporarily eliminated from consideration. In this model, Figure 1, straight biff-walls, i.e. walls without caps, of various heights, h_1, were placed at various distances, L_1, and tested at various values of the Froude Number, F_o. In all cases the Froude Number has been calculated on the basis of the mean jet velocity at the sluice outlet and the height of the sluice opening, so that

$$F_o = \frac{V_o^2}{gd_o} = \frac{q_o^2}{gd_o^3} \quad . \qquad (1)$$

Experiments were conducted over a Froude Number range from $F_o = 1$ to $F_o = 128$, a wall height range from $h_1 = 0.5d_o$ to $h_1 = 16d_o$ and a chamber length range from $L_1 = 2d_o$ to $L_1 = 64d_o$. To accomplish this, 245 runs were made and recorded photographically. Four regimes of flow were identified:

Condition A Submerged Flow
Condition B The Hydraulic Jump
Condition C The Forced Shock-Wave
Condition D The Spray Sheet or Unsubmerged Overflow.

Figure 2 indicates the type of flow obtained in each of the 245 runs together with groups of lines bounding the regimes of flow in the various "conditions".

The description, Condition A, was given to all flows in which the jet issuing from the sluice opening was submerged at the opening. Condition B includes only those runs in which the jet issued free from the sluice, passed through the true hydraulic jump in its full length, and flowed over the biff-wall in weir-type overflow. Condition C included those flows in which the jet issued free from the sluice outlet, passed through a standing shock-wave much like the hydraulic jump, and flowed

TWO-DIMENSIONAL STUDIES

Straight Bluff-Walls (Without Caps)

First, a two-dimensional model was constructed in which the lateral expansion from pipe to baffle box was temporarily eliminated from consideration. In this model, Figure 1, straight bluff-walls, i.e. walls without caps, of various heights, h', were placed at various distances, l', and tested at various values of the Froude Number, F^o. In all cases the Froude Number has been calculated on the basis of the mean jet velocity at the sluice outlet and the height of the sluice opening, so that

$$F^o = \frac{q^o}{A_s} = \frac{q^o}{g d_o^3} \qquad (1)$$

Experiments were conducted over a Froude Number range from $F^o = 1$ to $F^o = 120$, a wall height range from $h' = 0.84^o$ to $h' = 16^o$ and a chamber length range from $l' = 24^o$ to $l' = 64^o$. To accomplish this, 246 runs were made and recorded photographically. Four regimes of flow were identified:

Condition A Submerged Flow
Condition B The Hydraulic Jump
Condition C The Forced Shock-Wave
Condition D The Spray Sheet or Unsubmerged Overflow.

Figure 2 indicates the type of flow obtained in each of the 246 runs together with groups of lines bounding the regimes of flow in the various "conditions".

The description, Condition A, was given to all flows in which the jet issuing from the sluice opening was submerged at the opening. Condition B included only those runs in which the jet issued free from the sluice, passed through the true hydraulic jump in its full length, and flowed over the bluff-wall in weir-type overflow. Condition C included those flows in which the jet issued free from the sluice outlet, passed through a standing shock-wave much like the hydraulic jump, and flowed

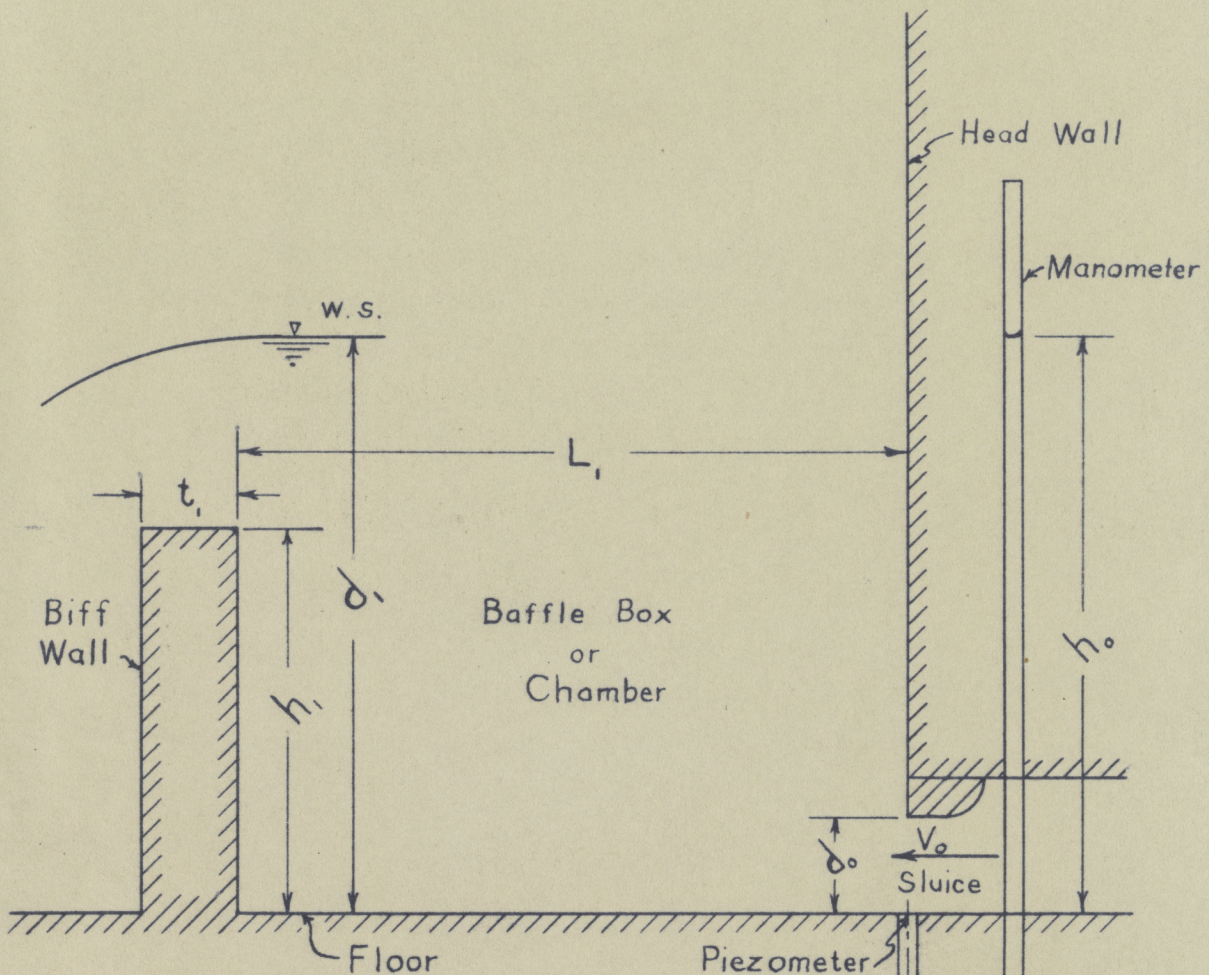

$$d_c = \left(\frac{V_o\, d_o}{\sqrt{g}}\right)^{\frac{2}{3}}$$

STRAIGHT WALL

SECTION THROUGH TWO-DIMENSIONAL MODEL

Fig. 1

over the biff-wall in leaping flow, i.e. flow with a stronger upward component than that of normal weir flow. Condition D included those flows which proceeded from the sluice opening over the biff-wall without submergence other than the small amount produced by the slowing down of the flow at the sides of the model, i.e. the rubber back-plate and the glass front window.

Condition A has been further subdivided into two regimes, A -short and A -long. In Condition A -long, as in Condition B, the flow over the biff-wall is weir-overflow. In Condition A -short, as in Condition C, the flow over the biff-wall is leaping overflow. In Figure 2 there is shown a family of lines which separate Condition A -short from Conditions A -long, B, and C. These lines have been constructed on the basis of an equation

$$L_1 = 5\,(d_1 - d_o) = 5\,(h_1 + Kd_o - d_o) \qquad (2)$$

which states that the minimum length of biff-wall chamber for any of the long conditions of flow is five times the difference between the depth of flow at the biff-wall and the height of the sluice opening. Since the depth of flow at the biff-wall is not directly predictable, the expression $h_1 + Kd_o$ in which K normally lies between 1 and 1.5 has been substituted for d_1. K may be computed from the weir coefficient as $K = \sqrt[3]{\frac{c}{C^2}}$. Equation 2 may be recognized as another form of a hydraulic-jump length equation suggested by Bakhmeteff and Matzke (Trans. Am. Soc.C.E. 101:643) in which $L_1 = C_1 \cdot d_j = C_1\,(d_1 - d_o)$ and C_1 has an approximate value of 5 over a wide range of F_o values. In the coordinates of Figure 2, Eq. 2 becomes

$$\frac{L_1}{h_1} = 5 + 5\,(K - F_o^{-\frac{1}{3}}) \cdot \frac{d_o}{h_1} \qquad (2a)$$

Conditions A -long and C are separated by the singular Condition B, which is obtainable only when the height h_1 is just sufficient to establish the conjugate depth corresponding to the particular values of d_o and F_o existing at the sluice outlet. Thus Condition B can only be

over the pitt-wall in leaping flow, i.e. flow with a stronger upward component than that of normal weir flow. Condition D involved those flows which proceeded from the sluice opening over the pitt-wall without appreciable submergence other than the small amount produced by the flowing down of the flow at the sides of the model, i.e. the rubber back-plate and the glass front window.

Condition A has been further subdivided into two regimes, A -short and A -long. In Condition A -long, as in Condition B, the flow over the pitt-wall is weir-overflow. In Condition A -short, as in Condition C, the flow over the pitt-wall is leaping overflow. In Figure 2 there is shown a family of lines which separate Condition A -short from Conditions A -long, B, and C. These lines have been constructed on the basis of an equation

$$I' = E\,(q' - q'_o) = E\,(p' + Kq'_o - q'_o) \qquad (2)$$

which states that the minimum length of pitt-wall chamber for any of the long conditions of flow is five times the difference between the depth of flow at the pitt-wall and the height of the sluice opening. Since the depth of flow at the pitt-wall is not directly predictable, the expression $p' + Kq'_o$ in which K normally lies between 1 and 1.5 has been substituted for q'. K may be computed from the weir coefficient as $K = \sqrt[3]{\frac{C_D}{E}}$. Equation 2 may be recognized as another form of a hydraulic-jump length equation suggested by Bakhmeteff and Matzke (Trans. Am. Soc.C.E. 101:662) in which $I' = C'J \cdot q'J = C'J\,(q' - q'_o)$ and $C'J$ has an approximate value of 5 over a wide range of p'_o values. In the coordinates of Figure 2, Eq. 2 becomes

$$\frac{p'}{I'} = E + E\,(K - p'_o - \frac{E}{I'}) \cdot \frac{p'}{q'_o} \qquad (2a)$$

Conditions A -long and C are separated by the singular Condition B, which is obtainable only when the height p' is just sufficient to establish the conjugate depth corresponding to the particular values of q'_o and p'_o emerging at the sluice outlet. Thus Condition B can only be

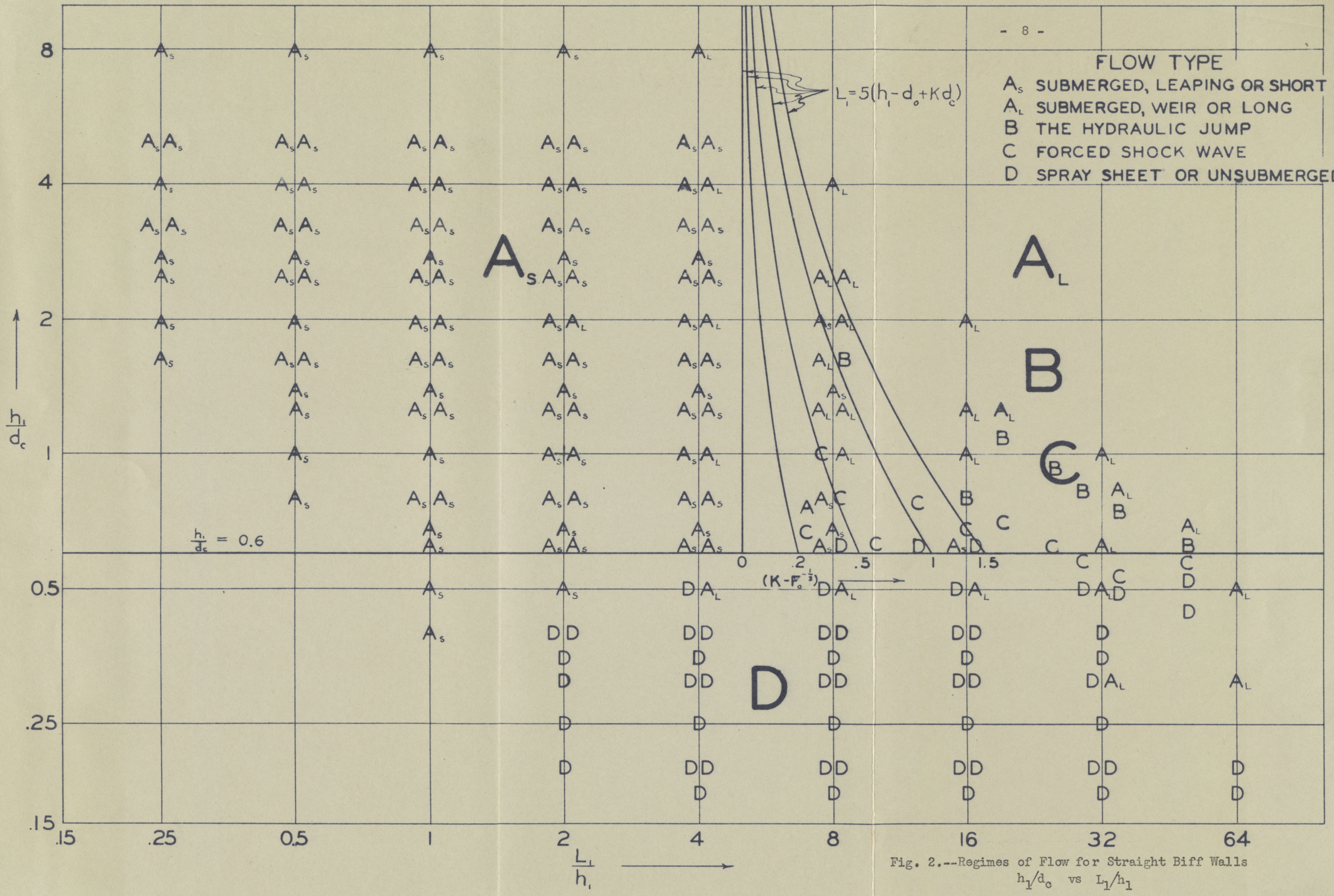

Fig. 2.--Regimes of Flow for Straight Biff Walls
h_1/d_c vs L_1/h_1

obtained at lower values of h_1 than those for Condition A -long and higher values of h_1 than those for Condition C. This fact is indicated in Figure 2 by the arrangement of the letters A_L, B, and C.

Conditions A -short and C are separated from Condition D by a critical value of the wall height such that

$$\frac{h_1}{d_c} = 0.6 .$$

Particular study was given to this quantity because of its significance in relation to stilling-pool depths (see Appendix A).

Photographs placed as Figures 3, 4, 5 and 6 show typical flow patterns for Conditions A, B, C and D respectively. It may be seen that, so long as there is sufficient length, L_1, for the development of Condition B, C, or D, length has no further effect on the performance of the flow upstream from the biff-wall. This fact is most effectively demonstrated by Figures 7 and 8 in which the loss coefficients for the various conditions of flow have been plotted.

In Figure 7, loss coefficients for Conditions A -long, B. C, and D have been plotted for lengths greater than those established by Eq. 2, as functions the height ratio $\frac{h_1}{d_c}$ and the Froude Number, F_o . The loss or dissipation of energy upstream from the biff-wall has been indicated on the chart by means of contours.

The loss coefficients were obtained by means of the Bernoulli equation

$$h_o + \frac{V_o^2}{2g} = d_1 + \frac{V_1^2}{2g} + h_{Loss} = d_1 + \frac{V_1^2}{2g} + C_L \cdot \frac{V_o^2}{2g} \qquad (3)$$

in the form

$$C_L = 1 - \frac{d_1 - h_o + \frac{V_1^2}{2g}}{\frac{V_o^2}{2g}} \qquad (4)$$

In practice $\frac{V_1^2}{2g}$ was neglected and the loss was computed as

$$C_L = 1 - \frac{d_1 - h_o}{\frac{V_o^2}{2g}} \qquad (4a)$$

obtained at lower values of h' than those for Condition A -long and higher values of h' than those for Condition C. This fact is indicated in Figure 2 by the arrangement of the letters A', B', and C.

Conditions A -short and C are separated from Condition D by a critical value of the weir height such that

$$\frac{q^o}{p_2} = 0.6 .$$

Particular study was given to this quantity because of its significance in relation to stilling-pool depths (see Appendix A).

Photographs placed as Figures 3, 4, 5 and 6 show typical flow patterns for Conditions A, B, C and D respectively. It may be seen that, so long as there is sufficient length, l', for the development of Condition B, C, or D, length has no further effect on the performance of the flow upstream from the drop-weir. This fact is most effectively demonstrated by Figures 7 and 8 in which the loss coefficients for the various conditions of flow have been plotted.

In Figure 7, loss coefficients for Conditions A -long, B, C, and D have been plotted for lengths greater than those established by Eq. 2, as functions the height ratio $\frac{q^o}{p_2}$ and the Froude Number, F^o. The loss or dissipation of energy upstream from the drop-weir has been indicated on the chart by means of contours.

The loss coefficients were obtained by means of the Bernoulli equation

$$y^o + \frac{\Sigma E}{\Delta S}{}^o = q^l + \frac{\Sigma E}{\Delta S}{}^l + h_{loss} = q^l + \frac{\Sigma E}{\Delta S}{}^s + C^l \cdot \frac{\Sigma E}{\Delta S}{}^s \qquad (2)$$

in the form

$$C^l = I - \frac{q^l - y^o + \frac{\Sigma E}{\Delta S}{}^l}{\frac{\Sigma E}{\Delta S}{}^o} \qquad (4)$$

In practice $\frac{\Sigma E}{\Delta S}{}^l$ was neglected and the loss was computed as

$$C^l = I - \frac{q^l - y^o}{\frac{\Sigma E}{\Delta S}{}^o} \qquad (4a)$$

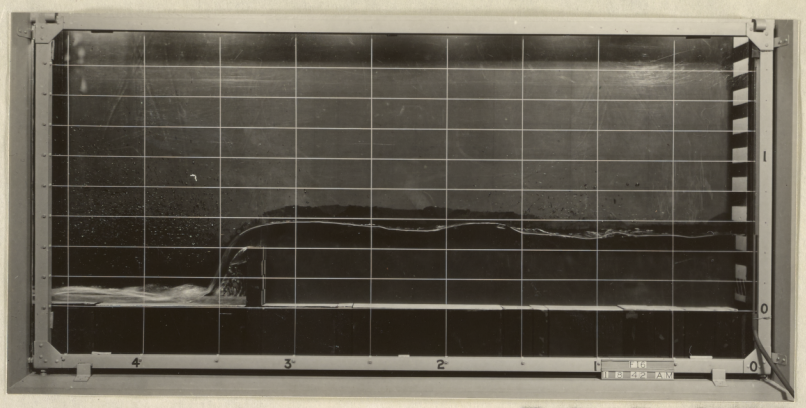

Photo. No. 1925-1

(a) Condition A -long. Weir Overflow

$$\underline{L_1 = 64d_o}$$

Diffusion of the jet is sufficiently complete for weir-type overflow at the biff-wall.

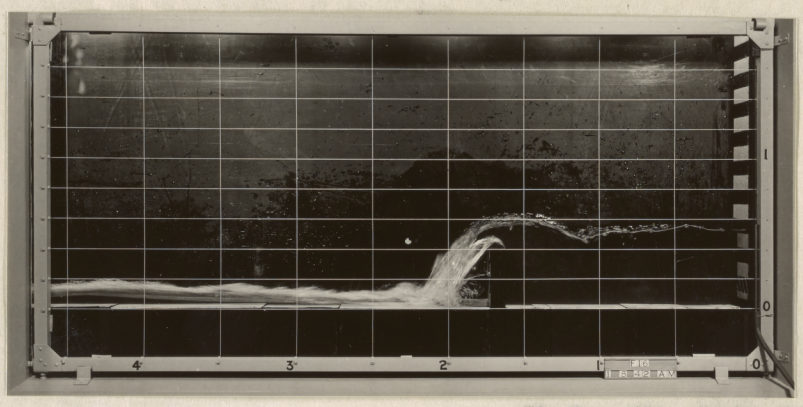

Photo. No. 1924-5

(b) Condition A -short. Leaping Overflow

$$\underline{L_1 = 32d_o}$$

FIGURE 5.---Condition A - SUBMERGED FLOW

A jet issues from a sluice opening of height, d_o = 0.05 ft., at F_o = 16, i.e. $\frac{V_o^2}{2g} = 8d_o$, and strikes a biff-wall of height $h_1 = 8d_o$, at two different distances, L_1.

Photo. No. 1988-1

(a) Condition A -long. Wall Overflow

$L^1 = 88\frac{1}{2}^0$

Diffusion of the jet is sufficiently complete for
wall-type overflow at the bilge-wall.

Photo. No. 1984-5

(b) Condition A -short. Leaping Overflow

$L^1 = 33\frac{1}{4}^0$

FIGURE 3.--Condition A - SUBMERGED FLOW

A jet issues from a sluice opening of height, $d^0 = 0.02$ ft., at $p^0 = 15^1$, i.e. $\frac{p^0}{d^0} = 84^0$, and strikes a bilge-wall of height $h^1 = 84^0$, at two different distances, L^1.

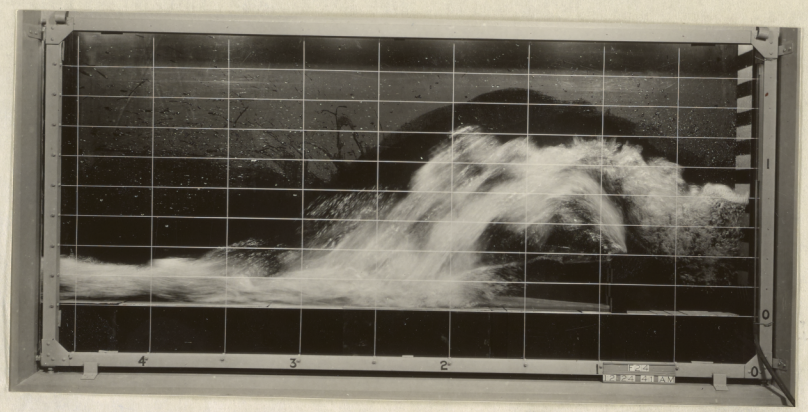

Photo. No. 1917-4

(c) $d_o = 0.10$ ft., $F_o = 24$, $h_1 = 4d_o$, $L_1 = 8d_o$

Note back pressure indicated by manometer

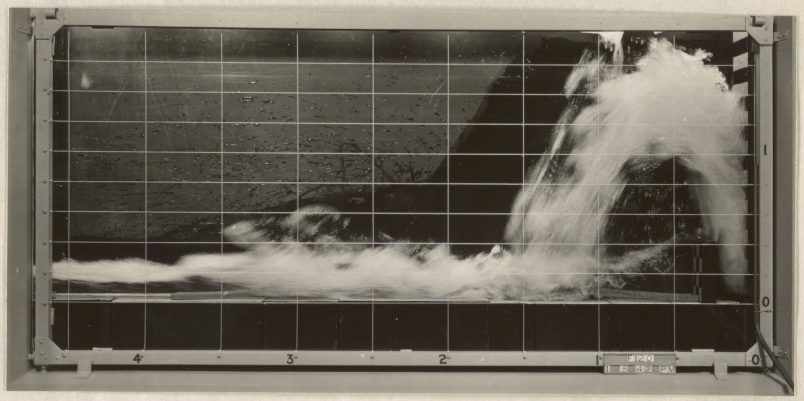

Photo. No. 1921-9

(d) $d_o = 0.05$ ft., $F_o = 120$, $h_1 = 8d_o$, $L_1 = 4d_o$

Note back pressure indicated by manometer

FIG. 3.---Condition A -Short

Deep Submergence and Strong Leaping Flow

Photo. No. 1917-C

(c) $d^{0} = 0.10$ ft., $\gamma^{0} = 24°$, $\gamma^{1} = 44°$, $I^{1} = 84°$

Note back pressure indicated by manometer

Photo. No. 1921-D

(d) $d^{0} = 0.08$ ft., $\gamma^{0} = 120°$, $\gamma^{1} = 84°$, $I^{1} = 44°$

Note back pressure indicated by manometer

FIG. 5.--Condition A -Short

Deep Submergence and Strong Leaping Flow

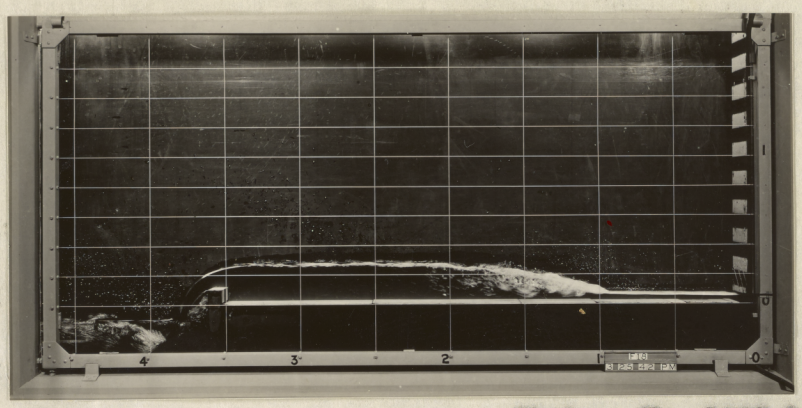

Photo. No. 1993-1

(a)

$F_o = 18$, $h_1 = 0.1$ ft. $= 2d_o$, $L_1 = 70d_o$

(Calculated conjugate depth, $d_2 = 0.276$ ft.)

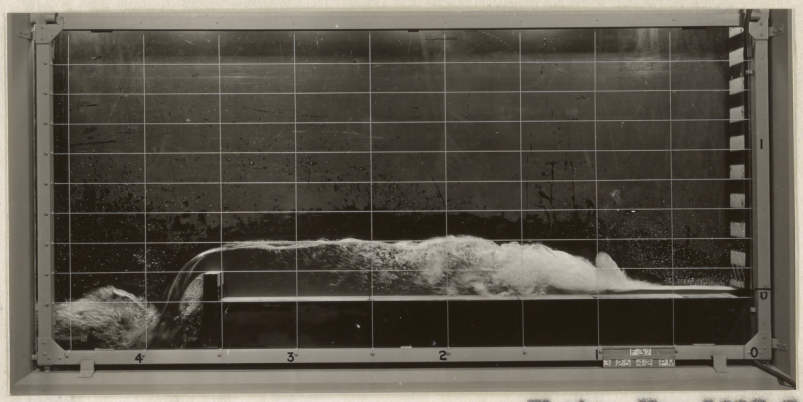

Photo. No. 1995-3

(b)

$F_o = 37$, $h_1 = 0.18$ ft. $= 3.6d_o$, $L_1 = 70d_o$

(Calculated conjugate depth, $d_2 = 0.407$ ft.)

FIG. 4.--Condition B - THE HYDRAULIC JUMP

A jet issues unsubmerged from a sluice opening of height $d_o = 0.05$ ft., passes through the hydraulic jump and over the biff wall placed at $L_1 = 3.5$ ft. for two different wall heights, h_1.

Photo. No. 1892-7

(a)

$P^0 = 18'$, $p^f = 0{\cdot}1$ lf. $= 24^0$, $I^f = 70^0$

(Calculated conjugate depth, $q^0 = 0{\cdot}2\%$ lf.)

Photo. No. 1892-8

(b)

$P^0 = 27'$, $p^f = 0{\cdot}18$ lf. $= 2{\cdot}8^0$, $I^f = 70^0$

(Calculated conjugate depth, $q^0 = 0{\cdot}40$ lf.)

FIG. 4.--Condition B - THE HYDRAULIC JUMP

the pitot meter placed at $I^f = 2{\cdot}8$ lf. for two different $q^0 = 0{\cdot}08$ lf.; passage through the hydraulic jump and over a jet issues submerged from a sluice opening of height

weir heights, p^f.

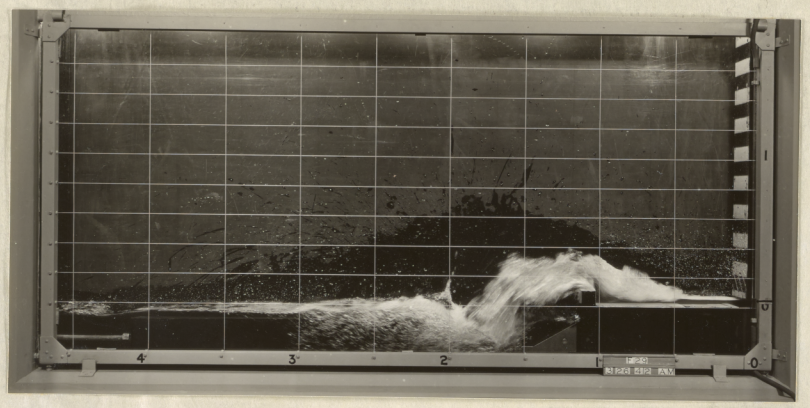

(a) Photo No. 1997-1

$F_o = 29$, $h_1 = 0.10$ ft. $= 2d_o$; $L_1 = 20d_o$.

$$\frac{h_1}{d_o} = .66$$

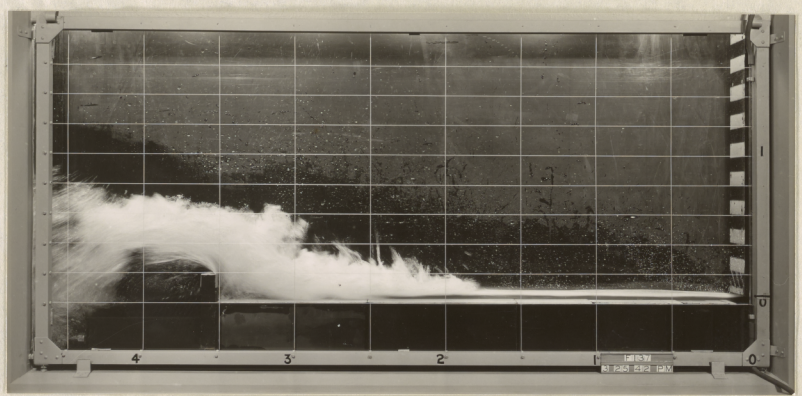

(b) Photo. No. 1995-4

$F_o = 137$; $h_1 = 0.18$ ft. $= 3.6d_o$; $L_1 = 70d_o$.

$$\frac{h_1}{d_o} = 0.70$$

Conditions identical with those of Figure 4b except for increase in F_o and d_o. The flow is unsubmerged for half the distance to the biff-wall.

FIG. 5.--Condition C - THE FORCED SHOCK-WAVE

An unsubmerged jet issues from a sluice opening of height, $d_o = 0.05$ ft., and forms a forced shock wave at the biff-wall.

(a) Photo No. 1307-1

$$\frac{p_j}{p_o} = .98$$

$M_o = 2.9$; $p_j = 0.10$ lb./in.^{2} abs.; $T_o = 524^\circ$; $T_j = 504^\circ$ abs.

(b) Photo. No. 1308-1

$$\frac{p_j}{p_o} = 0.10$$

$M_o = 1.97$; $p_j = 0.18$ lb./in.^{2} abs.; $T_o = 564^\circ$; $T_j = 704^\circ$ abs.

Conditions identical with those of Figure 6b except for increase in p_j and q_o. The flow is unsymmetrical for half the distance to the jet-wall.

FIG. 8.—Condition 6 — THE FORCED SHOCK-WAVE

An unsymmetrical jet issues from a slotted opening of height, $d_o = 0.02$ ft., and forms a forced shock wave at the jet-wall.

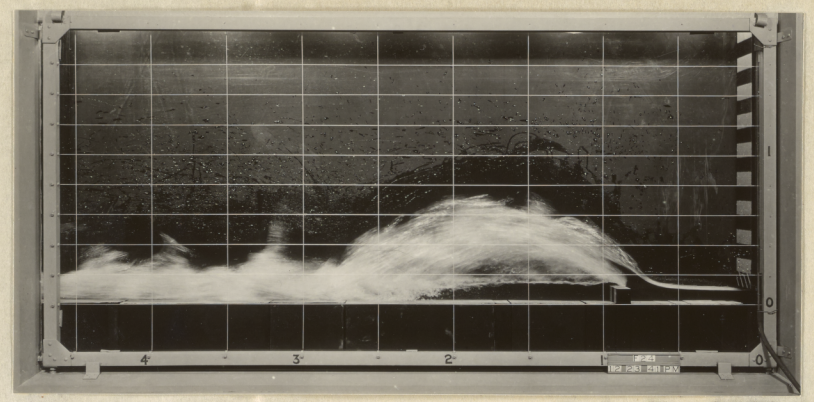

Photo No. 1907-4

(a)

$F_o = 24$, $h_1 = 0.10$ ft. $= d_o$; $L_1 = 8d_o$,

$$\frac{h_1}{d_o} = .35$$

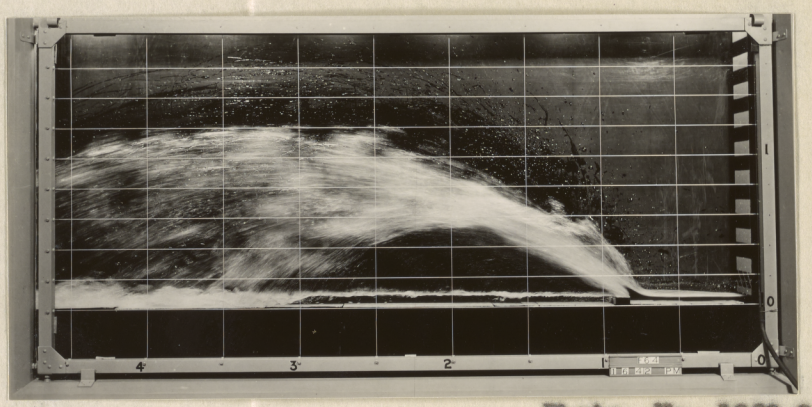

Photo. No. 1908-8

(b)

$F_o = 128^*$; $h_1 = 0.05$ ft. $= d_o$; $L_1 = 16d_o$,

$$\frac{h_1}{d_o} = .20$$

FIG. 6.---Condition D - THE SPRAY SHEET OR UNSUBMERGED OVERFLOW

A jet issues from a sluice opening of height, d_o, and proceeds unsubmerged over the biff-wall.

* Number on Photograph is in Error.

Photo No. 1504-4

(a) $h^0 = 124^*$; $p^f = 0.10$ ft. $= q^0$; $I^f = 84^0$.

$$\frac{q^0}{p^f} = .38$$

Photo. No. 1506-3

(b) $h^0 = 128^*$; $p^f = 0.05$ ft. $= q^0$; $I^f = 164^0$.

$$\frac{q^0}{p^f} = .20$$

FIG. 6.---Condition D - THE SHARP SHEET OR UNSUBMERGED OVERFLOW

A jet issues from a sluice opening of height q^0, and proceeds unsubmerged over the pitt-wall.

* Number on Photograph is in Error.

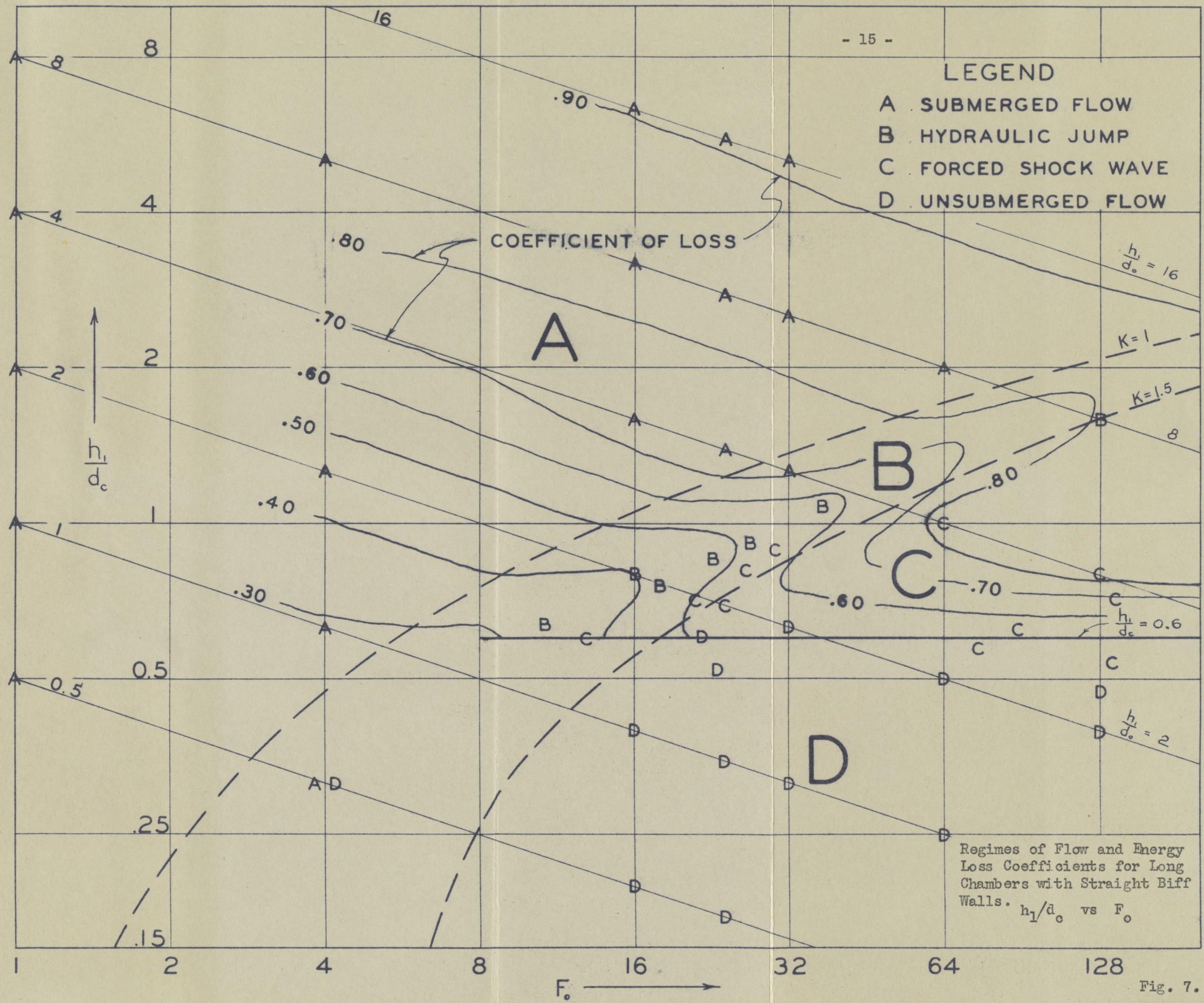

Regimes of Flow and Energy Loss Coefficients for Long Chambers with Straight Biff Walls. h_1/d_c vs F_o

Fig. 7.

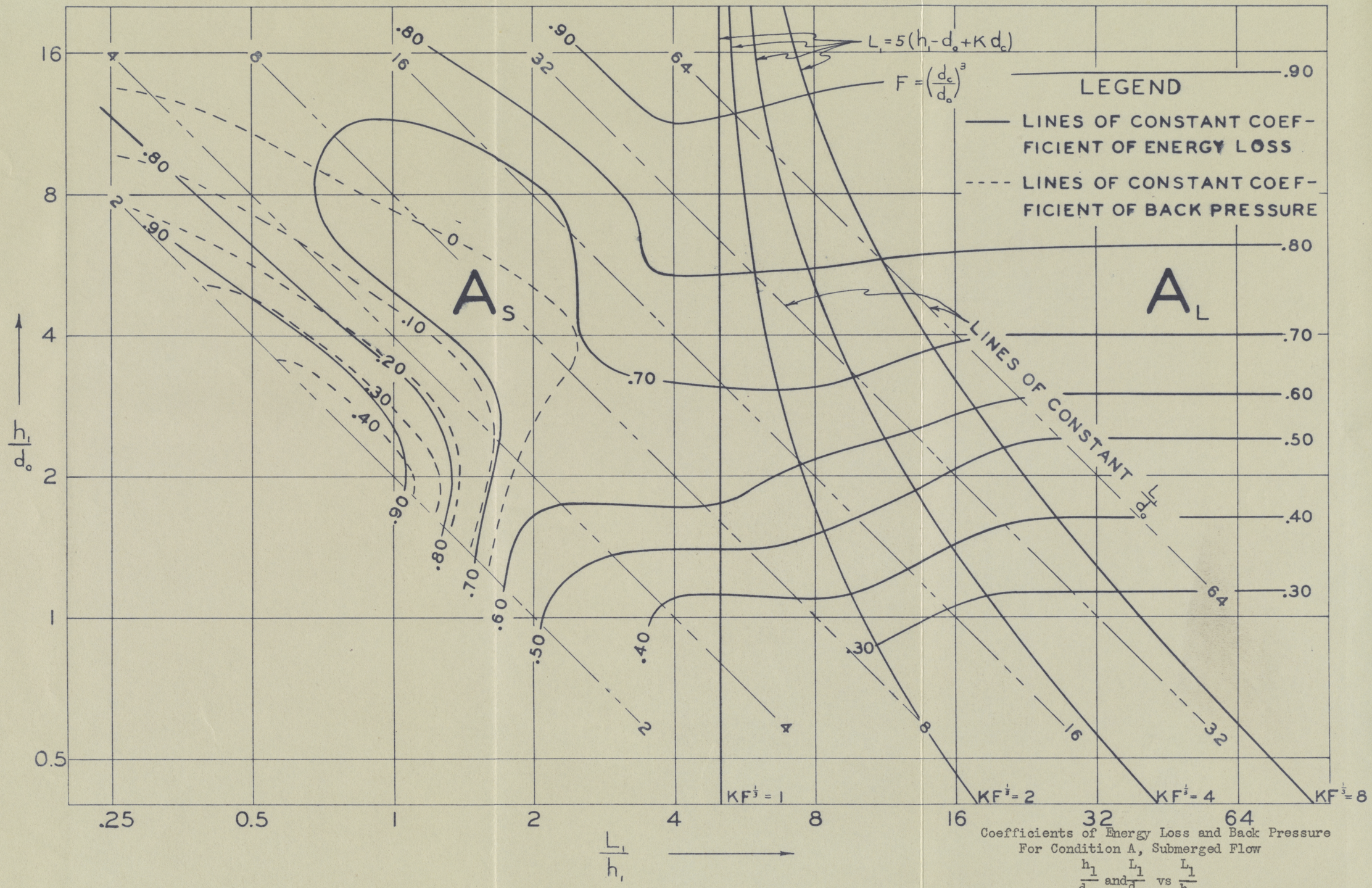

Coefficients of Energy Loss and Back Pressure
For Condition A, Submerged Flow
$\frac{h_1}{d_o}$ and $\frac{L_1}{d_o}$ vs $\frac{L_1}{h_1}$

Fig. 8.

Loss coefficients, obtained as above described, have been plotted in Figure 8 for Conditions A -short and A -long. Here the appropriate coordinates are another height ratio $\frac{h_1}{d_o}$ and a length ratio for the biff-wall chamber $\frac{L_1}{h_1}$. The parallel lines of constant loss coefficient in the A -long regime are equivalent to similar lines in Figure 7 shown parallel to the lines of constant $\frac{h_1}{d_o}$. Auxiliary lines of constant $\frac{L_1}{d_o}$ have been plotted in Figure 8 to indicate the effect of shortness of the chamber at low values of this ratio.

The use of Figures 7 and 8 for determining the values of the coefficients of energy loss and back pressure is illustrated by means of Table I. Columns 3 and 4 give values of the coefficients taken by interpolation from Figures 7 and 8. The values in columns 5 and 6 were determined directly by calculations based on observations from the photographs of the figures indicated in column 1.

TABLE I

Fig.	Condition	Figs. 7 and 8		Photograph	
		C_L	C_B	C_L	C_B
3a	A_L	0.84	0	0.81	-0.02
3b	A_s	0.84	0	0.81	-0.1
3c	A_s	0.71	0.03	0.72	-0.01
3d	A_s	0.77	0.07	0.73	0.04
4a	B	0.43	0	0.49	0
4b	B	0.58	0	0.62	0
5a	C	0.55	0	0.57	0
5b	C	0.60	0	0.80	0
6a	D	--- not determined ---			--
6b	D	--- not determined ---			--

C_L = Coefficient of Energy Loss

C_B = Coefficient of Back Pressure

loss coefficients, obtained as above described, have been plotted in Figure 8 for Conditions A -short and A -long. Here the appropriate coordinates are another height ratio $\frac{h_2}{d_o}$ and a length ratio for the diff-wall chamber $\frac{l_2}{d_o}$. The parallel lines of constant loss coefficient in the A -long regime are equivalent to similar lines in Figure 7 shown parallel to the lines of constant $\frac{h_2}{d_o}$. Auxiliary lines of constant $\frac{l_2}{d_o}$ have been plotted in Figure 8 to indicate the effect of shortness of the chamber at low values of this ratio.

The use of Figures 7 and 8 for determining the values of the coefficients of energy loss and back pressure is illustrated by means of Table I. Columns 3 and 4 give values of the coefficients taken by interpolation from Figures 7 and 8. The values in columns 5 and 6 were determined directly by calculations based on observations from the photographs of the figures indicated in column 1.

TABLE I

Fig.	Condition	Figs. 7 and 8 C_L	Figs. 7 and 8 C_B	Photographs C_L	Photographs C_B
5a	A_L	0.84	0	0.81	-0.02
5b	A_B	0.84	0	0.81	-0.1
5c	A_c	0.71	0.05	0.72	-0.01
5d	A_B	0.77	0.07	0.75	0.04
6a	H	0.45	0	0.49	0
6b	E	0.88	0	0.82	0
8a	C	0.85	0	0.87	0
8b	C	0.80	0	0.80	0
6a	D	---- not determined ----			---
6b	D	---- not determined ----			---

C_B = Coefficient of Back Pressure

C_L = Coefficient of Energy Loss

The velocity surveys of Figure 9 explain why the various loss contours of Figures 7 and 8 behave as they do. The measurements were made at Condition A -short, see Figure 10, although at a length approaching the critical value for change from A -short to A -long, see Figure 2. The approximate over-all loss coefficient for this performance was 86%, an amount comparing very favorably with that for $F_o = 58$, $h_1 = 8d_o$, $L_1 = 52d_o$ in Figures 7 and 8. As may be seen from the centerline velocity profiles and the loss coefficients derived therefrom, most of the loss took place through the spreading of the jet into the overlying water. Plotted with the experimental velocity profiles are theoretical velocity profiles based on pure jet-diffusion. The closeness of the solid bottom, and of the surface of the water also, to the top of the sluice opening explains the increased departure from the theory as the submerged jet proceeds downstream. The theory neglects both wall friction and upstream motion, presuming only that the jet diffuses into quiet water. In our experiment the upstream motion of the overlying water causes the jet to diffuse more rapidly and with greater loss than would the quiet water of very deep and vast submergence. The effect of bottom friction is seen in the curving of the lower end of each velocity profile.

If the biff wall of Figures 9 and 10 had been closer to the sluice outlet less energy would have been dissipated through diffusion and more through turning at the wall. According to Figure 8, a minimum value of total energy-loss would be reached at $\frac{L_1}{d_o} = 8$. As the length decreases further along the line of constant $\frac{h_1}{d_o} = 8$, the loss increases because the increase in turning loss more than takes the place of decrease in diffusion loss.

By means of Figures 2, 7 and 8, the regime of flow and the amount of energy dissipation for any combination of F_o, d_o, h_1, and L_1 can be determined. The nature of flow in the border zones between regimes A, B, C and D is shown in Figures 11, 12 and 13.

Any of these biff-wall systems may be used as an energy dissipating structure for a sluice outlet if a stilling-pool composed of an apron

The velocity surveys of Figure 9 explain why the various jets contours of Figures 7 and 8 behave as they do. The measurements were made at Condition A -short, see Figure 10, although at a length approaching the critical value for change from A -short to A -long, see Figure 2. The approximate over-all loss coefficient for this performance was 88%, an amount comparing very favorably with that for $P^o = 89$, $P^J = 84$, $I^J = 884$ in Figures 7 and 8. As may be seen from the centerline velocity profiles and the loss coefficients derived therefrom, most of the loss took place through the spreading of the jet into the overlying water. Plotted with the experimental velocity profiles are theoretical velocity profiles based on pure jet-diffusion. The closeness of the solid bottom, and of the surface of the water also, to the top of the sluice opening explains the increased departure from the theory as the submerged jet proceeds downstream. The theory neglects both wall friction and upstream motion, presuming only that the jet diffuses into quiet water. In our experiment the upstream motion of the overlying water causes the jet to diffuse more rapidly and with greater loss than would the quiet water of very deep and vast submergence. The effect of bottom friction is seen in the curving of the lower end of each velocity profile.

If the bluff wall of Figures 9 and 10 had been closer to the sluice outlet less energy would have been dissipated through diffusion and more through turning at the wall. According to Figure 8, a minimum value of total energy-loss would be reached at $\frac{d}{L^J} = 8$. As the length decreases further along the line of constant $\frac{h^o}{d^o} = 8$, the loss increases because the increase in turning loss more than takes the place of decrease in diffusion loss.

By means of Figures 2, 7 and 8, the regime of flow and the amount of energy dissipation for any combination of P^o, q^o, h^J, and L^J can be determined. The nature of flow in the border zones between regimes A, B, C and D is shown in Figures 11, 12 and 13.

Any of these bluff-wall systems may be used as an energy dissipating structure for a sluice outlet if a spilling-pool composed of an apron

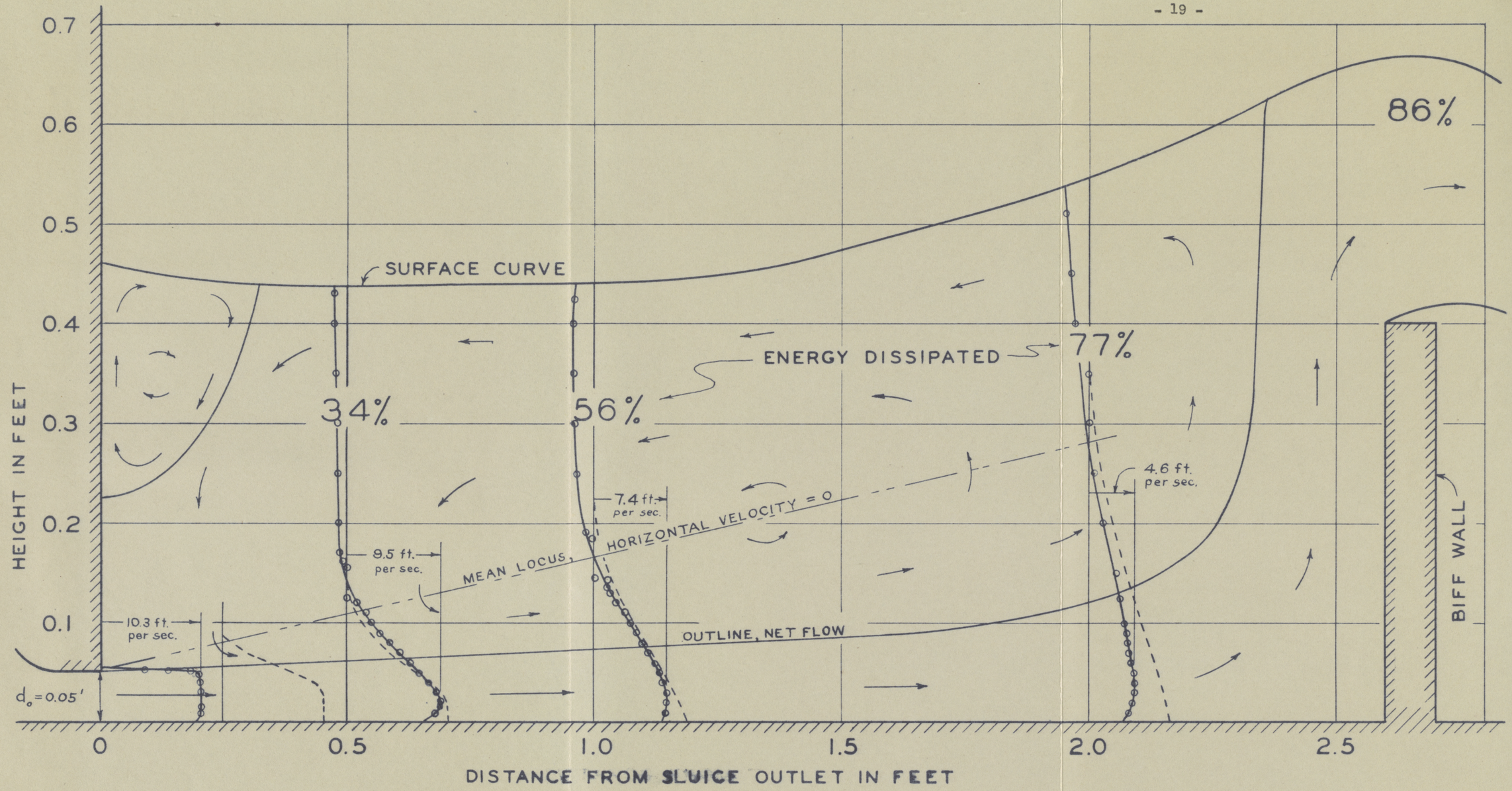

JET DIFFUSION SURVEY

$F_o = 58$

——●—●—● MEASURED VELOCITIES AT FLUME CENTER LINE.

– – – – – – THEORETICAL VELOCITIES (AFTER W. TOLLMIEN).

Fig. 9.

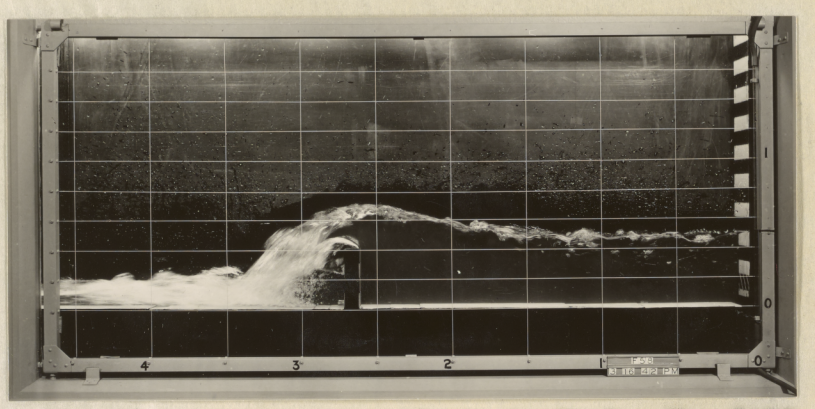

Photo. No. 1936

Condition A -Short

$d_o = 0.05$ ft., $F_o = 58$; $h_1 = 8d_o$, $L_1 = 52d_o$

FIG. 10.--PHOTOGRAPH OF THE JET DIFFUSION SURVEY

Photo. No. 1038

Condition A - Short

$d_0^0 = 0.05$ cm., $P_0^0 = 88$; $\beta_1^1 = 84^0$, $i_1^1 = 824^0$

FIG. 10.—PHOTOGRAPH OF THE 1ST DIFFUSION SURFACE

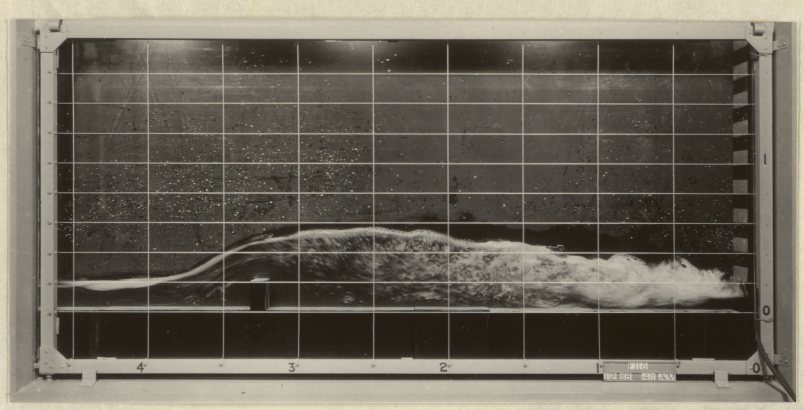

Photo. No. 1914-3

(a)

$$d_o = 0.10 \text{ ft.}; \; F_o = 16, \; h_1 = 2d_o; \; L_1 = 32d_o$$

The depth is slightly more than enough to produce the jump, but the flow approaches that of the jump. Compare with Figure 3b in which only the scale and the wall height are different.

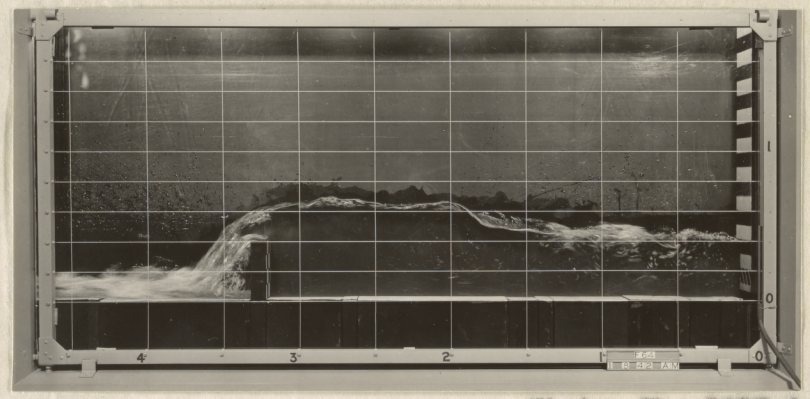

Photo. No. 1925-4

(b)

$$d_o = 0.05 \text{ ft.}; \; F_o = 64, \; h_1 = 8d_o; \; L_1 = 64d_o$$

Submergence is greater than Figure 11a but the condition lies between Figure 3a and Figure 4b.

Note slope of water surface. This flow is identical with conditions of Figure 3a except for increased Froude Number.

FIG. 11.--Condition A -long, approaching B - SHALLOW SUBMERGENCE

A high velocity jet issues from a sluice opening at the right, diffuses, and passes over the biff-wall in weir-type flow.

Photo. No. 1914-3

(a) $d^o = 0.10$ ft.; $F^o = 18$, $i^J = 84^o$; $i^J = 336^o$

The depth is slightly more than enough to produce the 'jump' but the flow approaches that of the 'jump.' Compare with Figure 8b in which only the scale and the wall height are different.

Photo. No. 1928-4

(b) $d^o = 0.08$ ft.; $F^o = 64$, $i^J = 84^o$; $i^J = 664^o$

Submergence is greater than Figure 11a but the condition lies between Figure 9a and Figure 4b.
Note slope of water surface. This flow is identical with conditions of Figure 8a except for increased Froude Number.

FIG. 11.--Condition A -'jump' approaching B - SHALLOW SUBMERGENCE weir-type flow.

A high velocity jet issues from a sluice opening at the right, diffuses, and passes over the diff-wall in

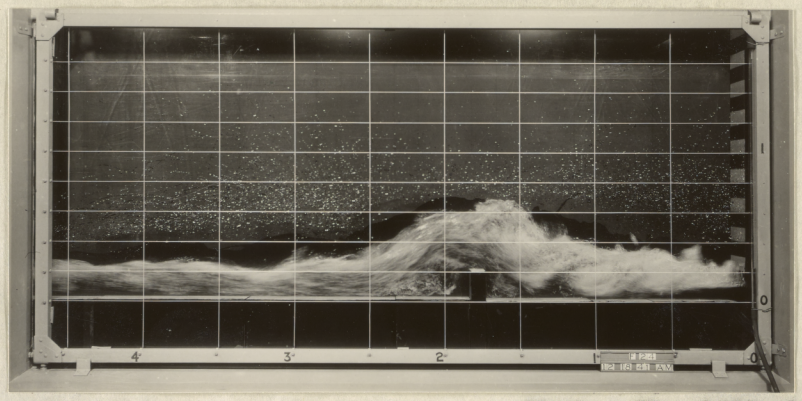

Photo. No. 1913-4

(a)

$d_o = 0.10$ ft.; $F_o = 24$; $h_1 = 2d_o$; $L_1 = 17d_o$

Submergence is so slight as to permit this performance to approach Condition C closely. Compare with Figure 5a.

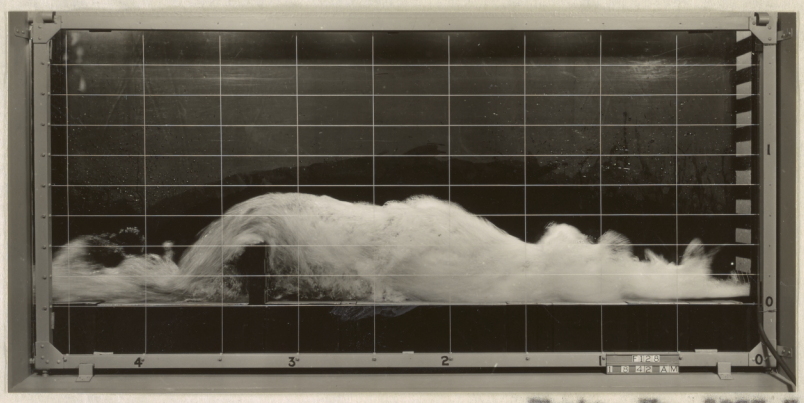

Photo. No. 1925-5

(b)

$d_o = 0.05$ ft.; $F_o = 128$; $h_1 = 8d_o$; $L_1 = 64d_o$

The length is only slightly less than that for the complete forced shock wave. Also the wall height is only slightly less than that for the hydraulic jump. Therefore, this is Condition A -short approaching Condition C, and, in turn, approaching Condition B.

Compare this condition with Figures 3a and 11b. All three are identical except for F_o.

FIG. 12.---Condition A -Short, Approaching Condition C.

SHALLOW SUBMERGENCE

Note Back Pressures Indicated by Manometer

(a)

$d_o^o = 0.10$ ft.; $P_o^o = 26$; $h_j^o = 24^o$; $L_j^o = 174^o$

Submergence is so slight as to permit this performance to approach Condition C closely. Compare with Figure 8a.

Photo. No. 1913-A

(b)

$d_o^o = 0.05$ ft.; $P_o^o = 132$; $h_j^o = 84^o$; $L_j^o = 664^o$

The length is only slightly less than that for the complete forced shock wave. Also the wall height is only slightly less than that for the hydraulic jump. Therefore, this is Condition A -short approaching Condition C, and, in turn, approaching Condition B.

Photo. No. 1928-B

Compare this condition with Figures 8a and 11b. All three are identical except for P_o^o.

FIG. 12.--Condition A -Short, Approaching Condition C.

SPECIAL SUBMERGENCE

Note Back Pressure Indicated by Manometer

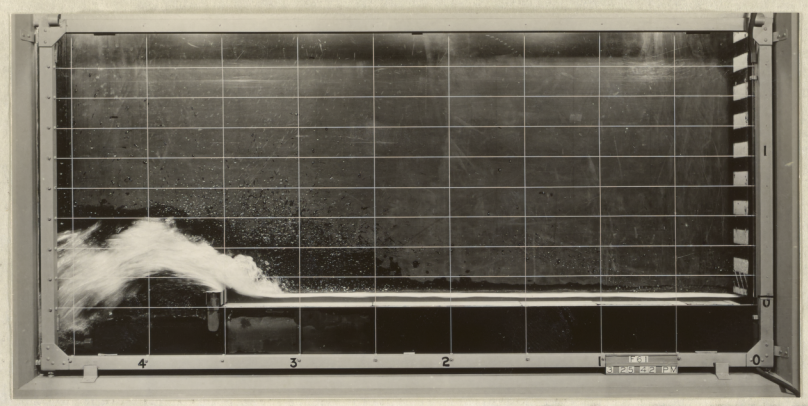

Photo. No. 1993-3

(a)

$F_o = 61$; $h_1 = 2d_o$; $L_1 = 70d_o$

$$\frac{h_1}{d_o} = 0.50$$

A slight increase in the velocity of the jet would remove the shock wave and "wash" the surface "clean" over the biff-wall crest. Compare this condition with Figure 4a, which is identical except for F_o.

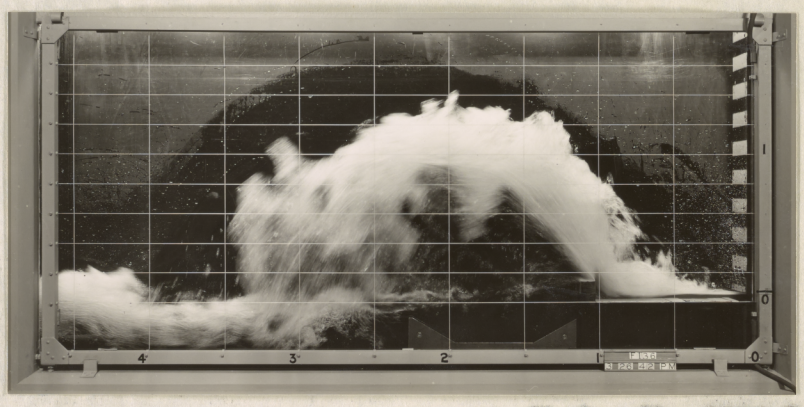

Photo. No. 1993-2

(b)

$F_o = 136$; $h_1 = .14$ ft. $= 2.8d_o$; $L_1 = 20d_o$

$$\frac{h_1}{d_o} = 0.53$$

Note strong leaping flow and submergence upstream from the biff-wall. At this value of F_o, the limiting quantity available, Condition D could not be obtained for $h_1 = 3d_o$.

FIG. 13.--Condition C (the short forced shock wave) Approaching Condition D

A High Velocity Jet Issues from a Sluice Opening of Height $d_o = 0.05$ ft.

(a) Photo. No. 1938-3

$P_o^1 = 81^\circ$; $\beta^1 = 24^\circ$; $L^1 = 704^\circ$

$$\frac{h_1}{d_o} = 0.80$$

A slight increase in the velocity of the jet would remove the shock wave and "wash" the surface "clean" over the *biff-wall* crest. Compare this condition with Figure 6e, which is identical except for P_o^1.

(b) Photo. No. 1939-3

$P_o^1 = 138$; $\beta^1 = 14$ ft. $= 2.8 d_o$; $L^1 = 204^\circ$

$$\frac{h_1}{d_o} = 0.88$$

Note strong leaping flow and submergence upstream from the *biff-wall*. At this value of P_o^1 the limiting quantity available. Condition D could not be obtained for $\beta^1 = 24^\circ$.

Fig. 12.---Condition C (the short forced shock wave)
Approaching Condition D

A High Velocity Jet Issues from a Sluice Opening of Height $d_o = 0.08$ ft.

and end-sill is used to dissipate energy and to direct the water flowing over the biff-wall. The photographs give some indication of the necessary length of apron since they show the shape of the nappe.

In applying a biff-wall structure to a particular outlet it is necessary to predict the amount of back pressure. For most cases of Condition A flow where $\frac{L_1}{d_o}$ is greater than 4, the back-pressure head may be calculated as

$$h_o = h_1 + Kd_c \qquad (5)$$

where $K = 1.5$ will be satisfactory for ordinary calculations. Where $\frac{L_1}{d_o}$ is small, the closeness of the wall increases the back-pressure and the following calculations should be used:

$$h_o = h_1 + Kd_c + C_B \cdot \frac{V_o^2}{2g} \qquad (5a)$$

or

$$h_o = h_1 + Kd_c + C_B \cdot \frac{F_o}{2} \cdot d_o \qquad (5b)$$

in which the coefficient of back-pressure, C_B, is taken from Fig. 8. In Conditions B, C, and D there is no back-pressure.

and end-sill is used to dissipate energy and to direct the water flowing over the bluff-wall. The photographs give some indication of the necessary length of apron since they show the shape of the nappe.

In applying a bluff-wall structure to a particular outlet it is necessary to predict the amount of back pressure. For most cases of Condition A flow where $\frac{q^o}{L_w}$ is greater than 4, the back-pressure head may be calculated as

$$p^o = p^1 + Kq^o \qquad (8)$$

where $K = 1.8$ will be satisfactory for ordinary calculations. Where $\frac{q^o}{L_w}$ is small, the closeness of the wall increases the back-pressure and the following calculations should be used:

$$p^o = p^1 + Kq^o + C^B \cdot \frac{\Sigma E^o}{A^2} \qquad (8a)$$

or

$$p^o = p^1 + Kq^o + C^B \cdot \frac{\Sigma}{L^o} \cdot q^o \qquad (8b)$$

In which the coefficient of back-pressure, C^B, is taken from Fig. 8. In Conditions B, C, and D there is no back-pressure.

TWO-DIMENSIONAL STUDIES

Capped Biff-Walls

In general, the structures required to return the flow from a straight biff-wall basin to the stream channel by means of an apron and end sill are fully as bulky as the hydraulic jump structure. Tests were made, therefore, to determine the effect of various lengths of cap on the size of structure required to handle a given flow as well as on the energy-dissipation characteristics of this type of wall.

In these tests it was found desirable to use a relatively large cap overhang in order to turn the flow back on itself completely, (see Fig. 26.) The length of cap overhang, x_1, has been determined by the relationship

$$x_1 = 0.5h_1 \qquad (6)$$

where h_1 is now the net height under the cap, (see Fig. 14). Complete reversal of the flow direction at the biff-wall produces two worthwhile effects. First, it forces diffusion to take place into a region of strong upstream velocity, thus diffusing the flow and dissipating energy rapidly. Second, it prevents leaping flow at the biff-wall, forcing the highest point in the overflow to be upstream rather than downstream from the biff-wall.

A definite height of biff-wall, h_1, is necessary to produce complete and uniform reversal of the flow. This height has a minimum value, $6d_o$, which obtains for the minimum distance from the head wall, $L_1 = 8d_o$. If the biff-wall is placed at greater distances from the sluice opening, greater heights are required to make up for the effect of rapid diffusion of the flow. The following relation is suggested for determining h_1

$$h_1 = 2d_o + \frac{1}{2} \cdot L_1 \qquad (7)$$

for $8 < \frac{L_1}{d_o} < 12$.

TWO-DIMENSIONAL STUDIES

Cropped Bluff-Walls

In general, the structures required to reduce the flow from a straight bluff-wall basin to the stream channel by means of an apron and end sill are fully as bulky as the hydraulic jump structure. Tests were made, therefore, to determine the effect of various lengths of cap on the size of structure required to handle a given flow as well as on the energy-dissipation characteristics of this type of wall.

In these tests it was found desirable to use a relatively large cap overhang in order to turn the flow back on itself completely. (see Fig. 28.) The length of cap overhang, x^1, has been determined by the relationship

$$x^1 = 0.8 y^1 \qquad (6)$$

where y^1 is now the net height under the cap, (see Fig. 14). Complete reversal of the flow direction at the bluff-wall produces two worthwhile effects. First, it forces diffusion to take place into a region of strong upstream velocity, thus diffusing the flow and dissipating energy rapidly. Second, it prevents leaping flow at the bluff-wall, forcing the highest point in the overflow to be upstream rather than downstream from the bluff-wall.

A definite height of bluff-wall, y^1, is necessary to produce complete and uniform reversal of the flow. This height has a minimum value, $6q^0$, which obtains for the minimum distance from the head wall, $L^1 = 8q^0$. If the bluff-wall is placed at greater distances from the sluice opening, greater heights are required to make up for the effect of rapid diffusion of the flow. The following relation is suggested for determining y^1

$$y^1 = 2q^0 + \frac{s}{5} \cdot L^1 \qquad (7)$$

for $8 \left\langle \frac{q^0}{y^1} \right\rangle 12$.

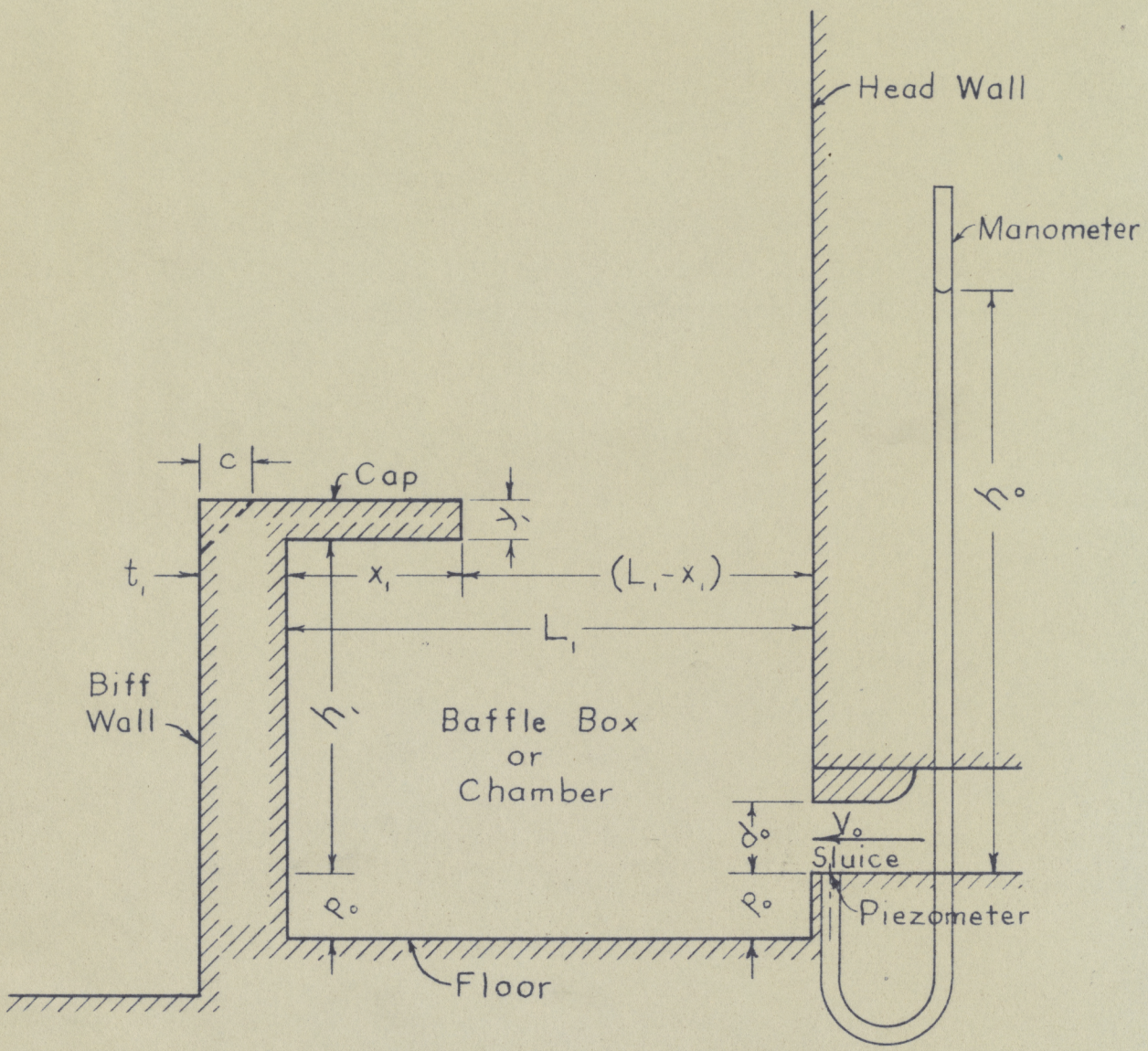

CAPPED WALL AND DEPRESSED FLOOR

SECTION THROUGH TWO-DIMENSIONAL MODEL

Fig. 14.

Having established x_1 and h_1 in terms of L_1 and d_o, we must still determine L_1 and the significance of F_o. For this purpose we must go to sketches prepared from the experiments, Figure 15. Three regimes of flow are evidently possible for structures based on equations 6 and 7 with various values of L_1 and F_o.

Where L_1 is large and F_o small, Type I flow occurs. In this regime the head or depth of overflow required to maintain flow over the biff-wall is sufficient to reverse the flow direction at the upstream-edge of the cap.

At larger values of F_o or smaller values of L_1, Type II flow is obtained. This is the condition regarded as most desirable for biff-wall structures. The head required to remove the water from the structure is no longer sufficient to turn the water before it reaches the head wall in its upstream motion. The distance L_1 is small compared with that necessary for Type I flow.

Further increase in F_o or decrease in L_1 produces Type III flow. In this condition the water rising at the head wall and falling again does not strike the top of the biff-wall on its way down. There are three disadvantages in this type of flow as compared with Type II. First, the height of side wall required is great compared with the height of biff-wall. Second, the freely falling nappe, not being in contact with the rising flow, has no opportunity to diffuse with it. Third, the air entrainment opportunities are greater in Type III than in Type II.

In Type II flow the principal flow is in contact with a wall or, better yet, with a current of water traveling in the opposite direction, through a very large fraction of its whole path length. Type II flow is, therefore, a very effective energy-dissipating system producing both large diffusion losses and large bend losses.

A chart, Figure 16, shows the ranges of F_o and $\frac{L_1}{d_o}$ in which the various types of flow are developed. From this chart an equation may be written such that Type II flow can always be secured with a minimum structure size:

Having established x^1 and h^1 in terms of l^1 and q^o, we must still determine l^1 and the significance of k^o. For this purpose we must go to sketches prepared from the experiments, Figure 18. Three regimes of flow are evidently possible for structures based on equations 6 and 7 with various values of l^1 and k^o.

Where l^1 is large and k^o small, Type I flow occurs. In this regime the head or depth of overflow required to maintain flow over the pitt-wall is sufficient to reverse the flow direction at the upstream-edge of the cap.

At larger values of k^o or smaller values of l^1, Type II flow is obtained. This is the condition regarded as most desirable for pitt-wall structures. The head required to remove the water from the structure is no longer sufficient to turn the water before it reaches the head wall in its upstream motion. The distance l^1 is small compared with that necessary for Type I flow.

Further increase in k^o or decrease in l^1 produces Type III flow. In this condition the water rising at the head wall and falling again does not sprize the top of the pitt-wall on its way down. There are three disadvantages in this type of flow as compared with Type II. First, the height of side wall required is great compared with the height of pitt-wall. Second, the freely falling nappe, not being in contact with the rising flow, has no opportunity to diffuse with it. Third, the air entrainment opportunities are greater in Type III than in Type II.

In Type II flow the principal flow is in contact with a wall or better yet, with a current of water traveling in the opposite direction, through a very large fraction of its whole path length. Type II flow is, therefore, a very effective energy-dissipating system producing both large diffusion losses and large bend losses.

A chart, Figure 19, shows the ranges of k^o and $\frac{q^o}{l^1}$ in which the various types of flow are developed. From this chart an equation may be written such that Type II flow can always be secured with a minimum structure size:

(a)

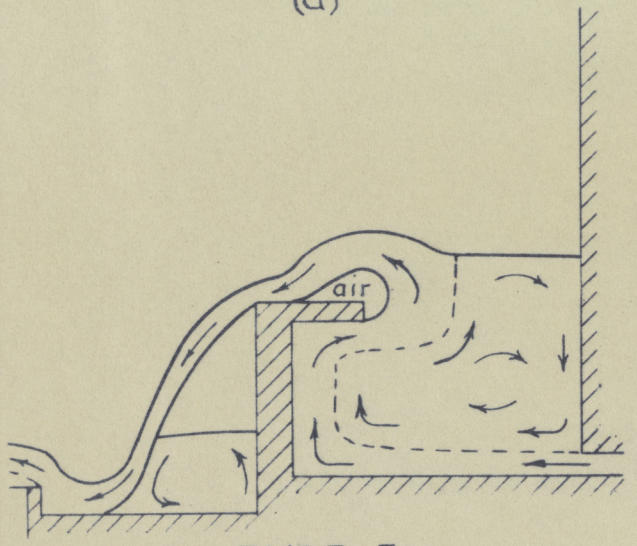

TYPE I

$F_o = 24$; $\frac{h_1}{d_o} = 8$; $\frac{x_1}{d_o} = 4$; $\frac{L_1}{d_o} = 13$

Wall higher and chamber longer than necessary.

(b)

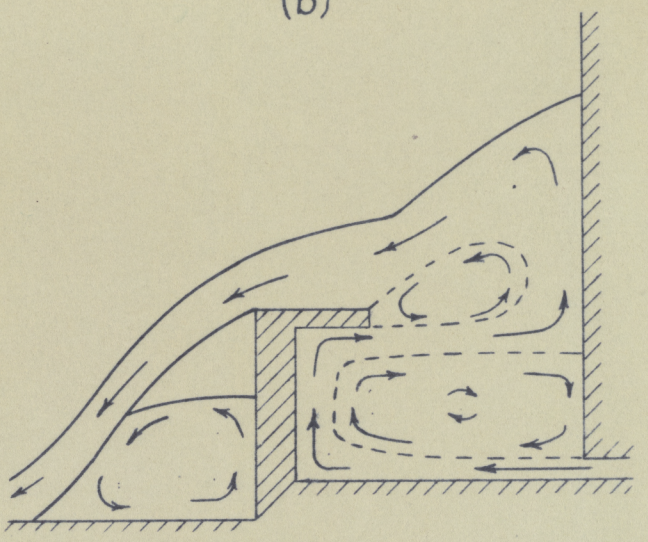

TYPE II

$F_o = 100$; $\frac{h_1}{d_o} = 8$; $\frac{x_1}{d_o} = 4$; $\frac{L_1}{d_o} = 13$

Design dimensions adequate, but possibly smaller structure would perform satisfactorily.

(c)

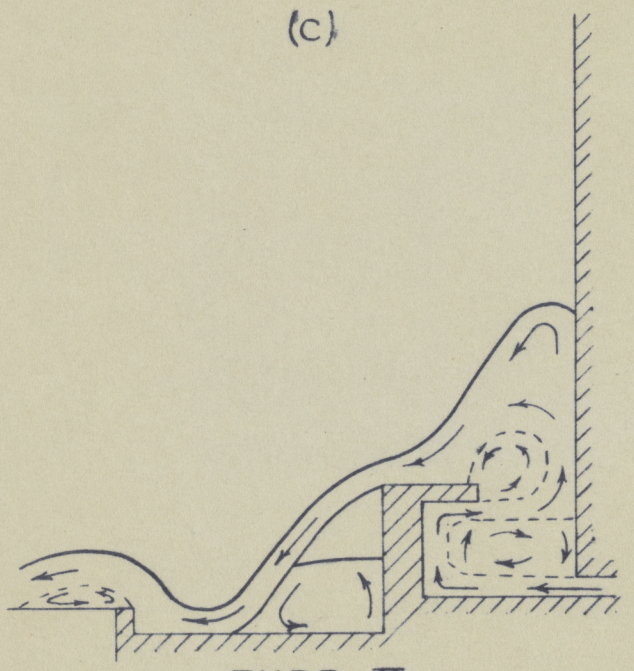

TYPE II

$F_o = 24$; $\frac{h_1}{d_o} = 6$; $\frac{x_1}{d_o} = 3$; $\frac{L_1}{d_o} = 8$

Structure properly designed for given flow rate. Minimum dimensions for good performance.

(d)

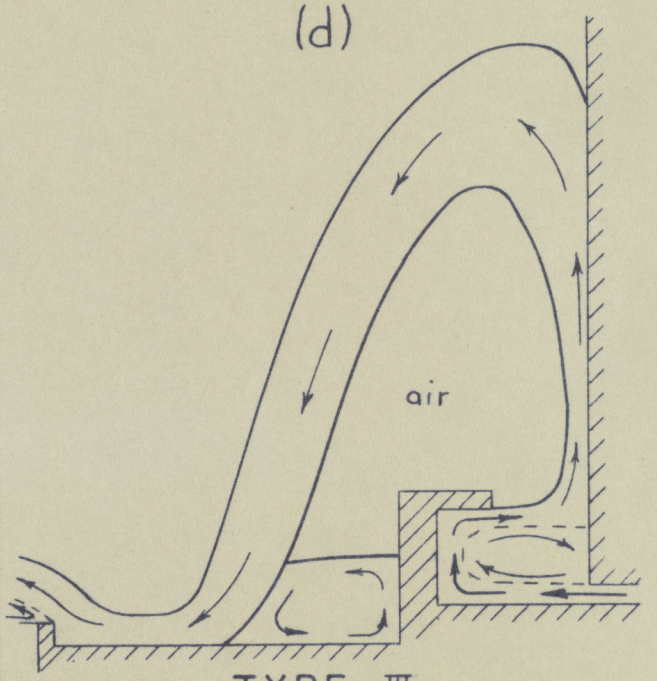

TYPE III

$F_o = 100$; $\frac{h_1}{d_o} = 6$; $\frac{x_1}{d_o} = 3$; $\frac{L_1}{d_o} = 8$

Structure greatly overloaded. Air entrainment excessive, and very high side walls required.

Froude Numbers, F_o, are Estimated

Flow Sketches for Regimes of Flow For Capped Biff Walls

Fig. 15.

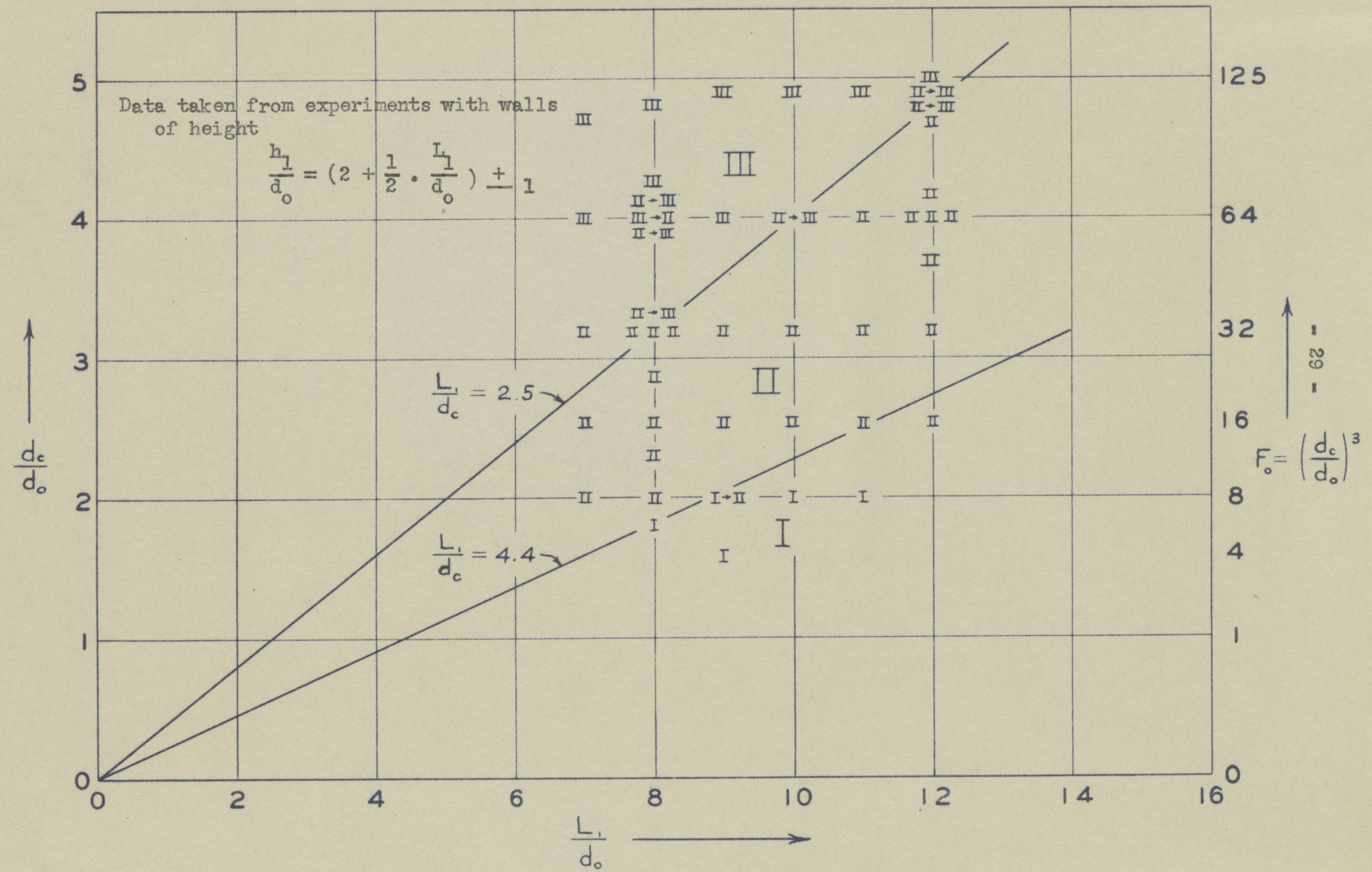

Fig. 16.---Regimes of Flow-Capped Biff-Walls

$$\frac{L_1}{d_o} = 2.5\,(F_o)^{\frac{1}{3}} = 2.5\,\frac{d_c}{d_o} \qquad (8)$$

or

$$\frac{L_1}{d_c} = 2.5 \qquad (8a)$$

A similar equation $\frac{L_1}{d_c} = 4.4$ may be used to separate Type I from Type II. (9)

If a structure is designed by means of equation 8a, it will operate in Type II flow at high discharges and Type I at low. A stilling pool may be proportioned to suit the overfall trajectory from the biff-wall. Laboratory studies indicate that the stilling pool length may be determined either by the maximum rate of flow or by a rate, say $F = \frac{1}{3} F_{max}$, at which the nappe projects farthest from the wall.

It now may be noted that the unit discharge,

$$q = V_o d_o = d_c \sqrt{g d_c} = d_c \sqrt{F_o g d_o}$$

enters into the determination of wall requirement and structure performance, directly in the length, L_1, and only indirectly in the height of wall h_1 and the cap overhang x_1. This fact is of great significance; it indicates that, so long as any one type of flow is obtained, energy dissipation and flow stability are determined by the geometry of the biff-wall alone. The same height of biff-wall will handle all flows so long as increased length is not needed to keep the performance within Type II. Even then, only a small increase in wall height is required to take into account expansion of the jet through diffusion.

Tests were made with square-crested walls and with chamfered walls. By permitting shorter nappe trajectories and shorter structures chamfered walls can be used to advantage and are, therefore, recommended.

Photographs of performances of all three types and at several Froude Numbers are included in this report, (see Figs. 17 through 21).

$$\frac{q^o}{\Gamma^J} = 2.8 \left(\Gamma^o\right)^{\frac{2}{J}} = 2.8 \frac{q^o}{q^o} \qquad (8)$$

or

$$\frac{q^o}{\Gamma^J} = 2.8 \qquad (8a)$$

A similar equation $\frac{q^o}{\Gamma^J} = \epsilon \cdot \epsilon$ may be used to separate Type I from Type II.

If a structure is designed by means of equation 8a, it will operate in Type II flow at high discharges and Type I at low. A stilling pool may be proportioned to suit the overfall trajectory from the pitt-wall; laboratory studies indicate that the stilling pool length may be determined either by the maximum rate of flow or by a rate, say $\beta = \frac{2}{J}\beta^{max}$, at which the nappe projects furthest from the wall.

It now may be noted that the unit discharge,

$$d = A^o q^o = q^o \sqrt{Lg^o} = q^o \sqrt{L^o g^o}$$

enters into the determination of wall reinforcement and structure performance, directly in the length, Γ^J, and only indirectly in the height of wall β^J and the cap overhang κ^J. This fact is of great significance; it indicates that, so long as any one type of flow is obtained, energy dissipation and flow stability are determined by the geometry of the pitt-wall alone. The same height of pitt-wall will handle all flows so long as increased length is not needed to keep the performance within Type II. Even then, only a small increase in wall height is required to take into account expansion of the jet through diffusion.

Tests were made with square-crested walls and with chamfered walls. By permitting shorter nappe trajectories and shorter structure clearance, chamfered walls can be used to advantage and are, therefore, recommended.

Photographs of performance of all three types and at several Froude Numbers are included in this report (see Figs. IX through 21).

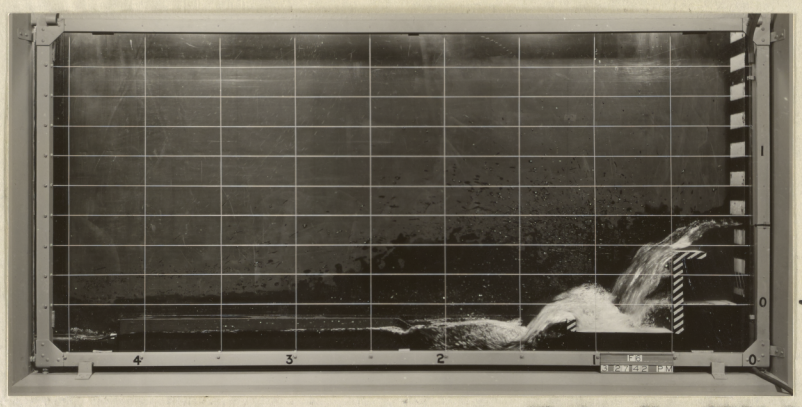

Sluice Opening
d_o = 0.05 ft.

Photo. No. 2100-1

(a)

$$F_o = 6,\ h_1 = 6d_o,\ L_1 = 8d_o,\ x_1 = 3d_o$$

Compare with Figures 18a and 18b, in which only Froude Number is changed.

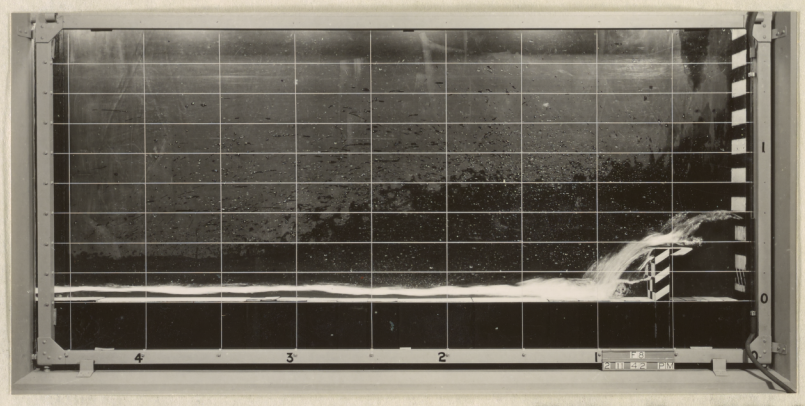

Sluice Opening
d_o = 0.05 ft.

Photo. No. 1956-1.

(b)

$$F_o = 8,\ h_1 = 6d_o,\ L_1 = 10d_o,\ x_1 = 3d_o$$

Compare with Figure 20c in which only F_o is changed.

FIG. 17.--TYPE I FLOW

This Type of Pattern Occurs at Relatively Low Discharges.

Slusoe Opening
d^0 = 0.05 ft.

Photo. No. 21300-J

(a) $P^0 = 6^0$, $P^1 = 84^0$, $I^1 = 84^0$, $x^1 = 24^0$

Compare with Figures 18a and 18b, in which only Fronde Number is changed.

Slusoe Opening
d^0 = 0.05 ft.

Photo. No. 1886-J.

(b) $P^0 = 8^0$, $P^1 = 64^0$, $I^1 = 104^0$, $x^1 = 24^0$

Compare with Figure 20a in which only P^0 is changed.

FIG. 17.--TYPE I FLOW

This Type of Pattern Occurs at Relatively low Discharges.

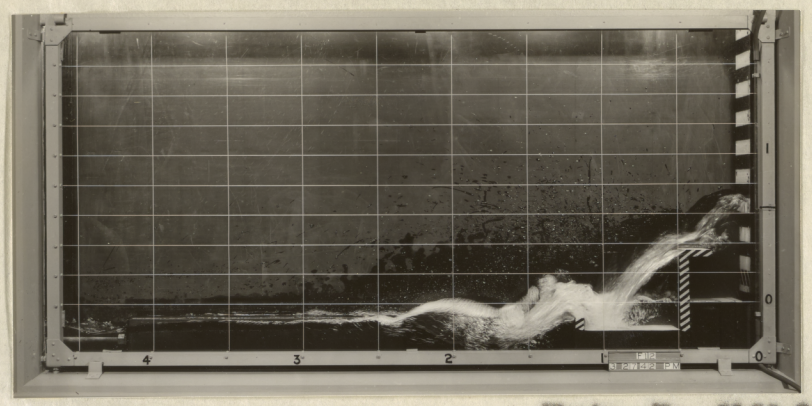

← Sluice Opening d_o = 0.05 ft.

Photo. No. 2100-2

(a)

Type II - Low Velocity

$F_o = 12$, $h_1 = 6d_o$, $L_1 = 8d_o$, $x_1 = 3d_o$

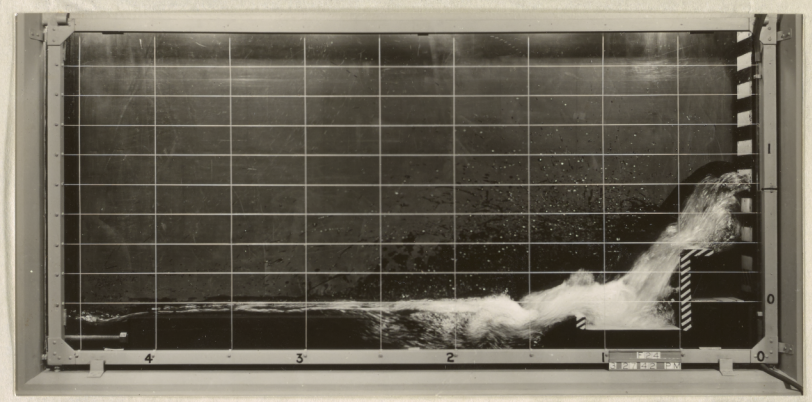

← Sluice Opening d_o = 0.05 ft.

Photo. No. 2100-3

(b)

Type II Flow - Recommended Performance

$F_o = 24$, $h_1 = 6d_o$, $L_1 = 8d_o$, $x_1 = 3d_o$

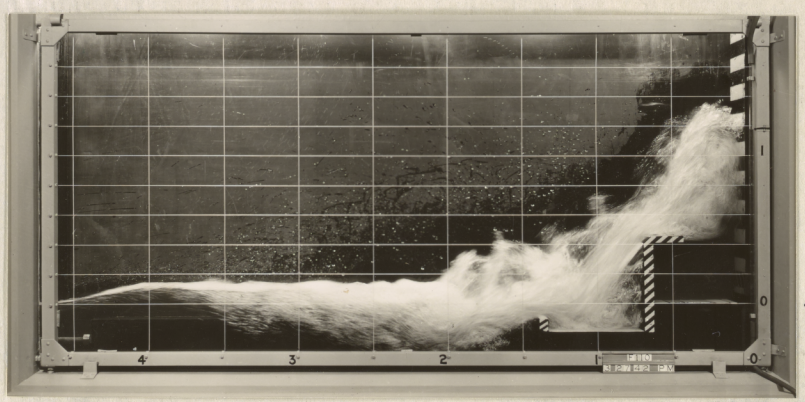

← Sluice Opening d_o = 0.05 ft.

Photo. No. 2102-3

(c)

Type II Flow - Good Performance

$F_o = 110$, $h_1 = 8d_o$, $L_1 = 12d_o$, $x_1 = 4d_o$

FIG. 18.--TYPE II FLOW - Structures Shown Above are all Satisfactory Energy Dissipators.

Photo. No. 2100-2

(a) Type II - Low Velocity

$F^o = 12°$, $\beta^1 = 64^o$, $\Gamma^1 = 24^o$, $\alpha^1 = 24^o$

Photo. No. 2100-3

(b) Type II Flow - Recommended Performance

$F^o = 24°$, $\beta^1 = 64^o$, $\Gamma^1 = 84^o$, $\alpha^1 = 84^o$

Photo. No. 2102-3

(c) Type II Flow - Good Performance

$F^o = 110°$, $\beta^1 = 84^o$, $\Gamma^1 = 124^o$, $\alpha^1 = 44^o$

FIG. 18.--TYPE II FLOW - Structures Shown Above are all Satisfactory Inserts.
Dissipators.

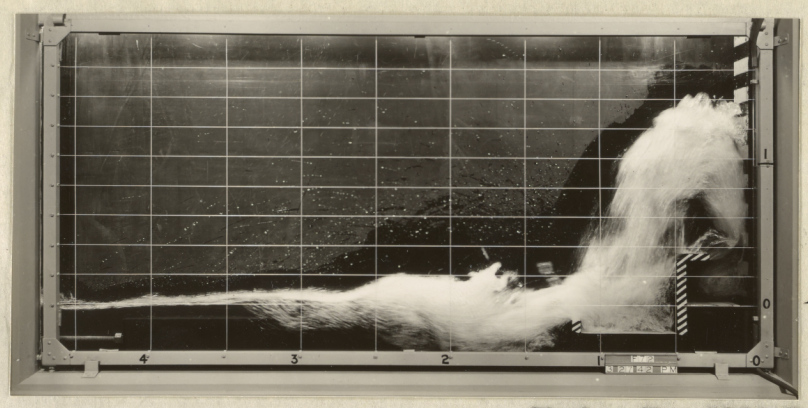

Sluice Opening
d_o = 0.05 ft.

Photo. No. 2100-5

(a)

$F_o = 72$, $h_1 = 6d_o$, $L_1 = 8d_o$, $x_1 = 3d_o$

Compare with Figures 17a, 18a, and 18b.
Only the Froude Number is changed.

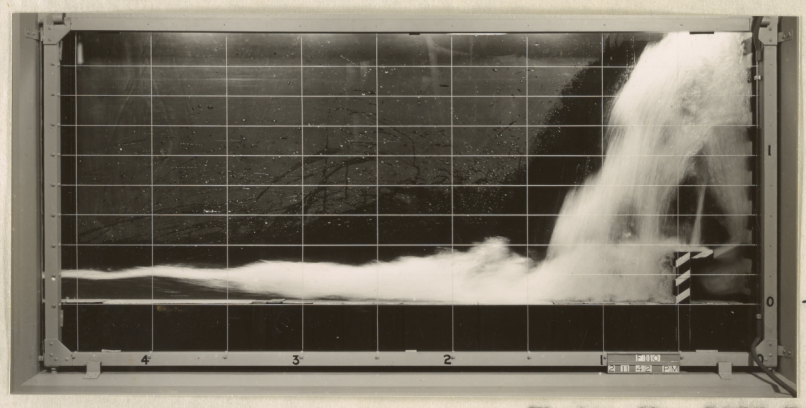

Sluice Opening
d_o = 0.05 ft.

Photo. No. 1955-5

(b)

$F_o = 110$, $h_1 = 6d_o$, $L_1 = 8d_o$, $x_1 = 3d_o$

Froude Number increased still more.

FIG. 19.--TYPE III FLOW

Note large amount of air entrainment and high side walls required.

Sluice Opening
d^0 = 0.05 ft.

(a)

$\gamma^0 = 72°$, $i^1 = 84^0$, $L^1 = 84^0$, $x^1 = 84^0$

Photo. No. 2100-S

Compare with Figures IVa, IBa, and IBb.
Only the Froude Number is changed.

Sluice Opening
d^0 = 0.05 ft.

(b)

$\gamma^0 = 110°$, $i^1 = 84^0$, $L^1 = 84^0$, $x^1 = 84^0$

Photo. No. 1909-S

Froude Number increased still more.

FIG. 19.—TYPE III FLOW

Note large amount of air entrainment and high slope wall required.

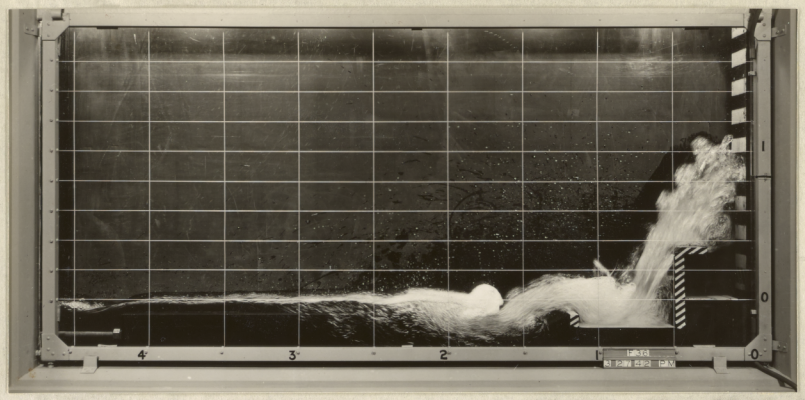

Sluice Opening
d_o = 0.05 ft.

Photo. No. 2100-4

(a) Type II → III Flow.

Design by Eq. 8 would permit F_o = 32.
F_o = 36, $h_1 = 6d_o$, $L_1 = 8d_o$, $x_1 = 3d_o$
Compare with Figures 18, a,b, and Figure 19a.

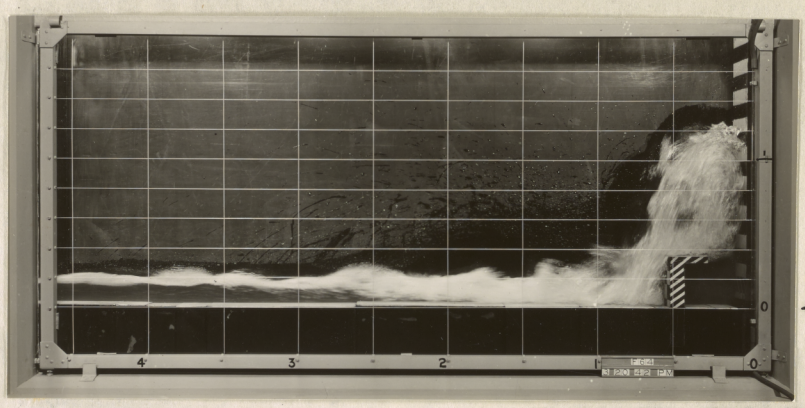

Sluice Opening
d_o = 0.05 ft.

Photo. No. 1955-8

(b) Type III → II Flow - Structure Overloaded.
F_o = 64, $h_1 = 6d_o$, $L_1 = 8d_o$, $x_1 = 3d_o$

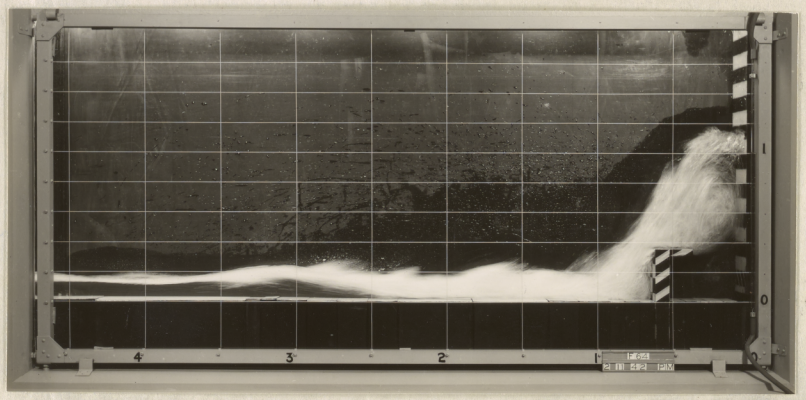

Sluice Opening
d_o = 0.05 ft.

Photo. No. 1956-4

(c) Type III → II Flow - Structure Somewhat Overloaded
F_o = 64, $h_1 = 6d_o$; $L_1 = 10d_o$; $x_1 = 3d_o$. Design by Eq. 6,7 and 8 would furnish $h_1 = 7d_o$ and $x_1 = 3.5d_o$

FIG. 20.—TYPE II Approaching III, and TYPE III Approaching II FLOWS

Sluice Opening
d^o = 0.08 ft.

(a)

Sluice Opening
d^o = 0.08 ft.

(b)

Sluice Opening
d^o = 0.08 ft.

(c)

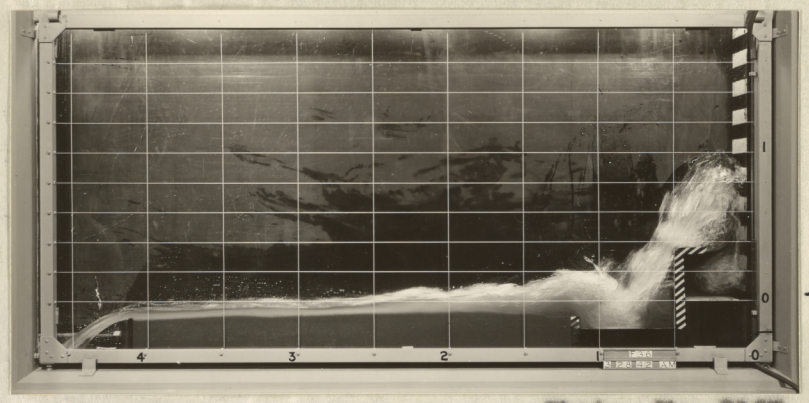

Sluice Opening
d_o = 0.05 ft.

Photo. No. 2105

(a) $F_o = 36$, $h_1 = 6d_o$, $L_1 = 8d_o$, $x_1 = 3d_o$

Discharge begins.

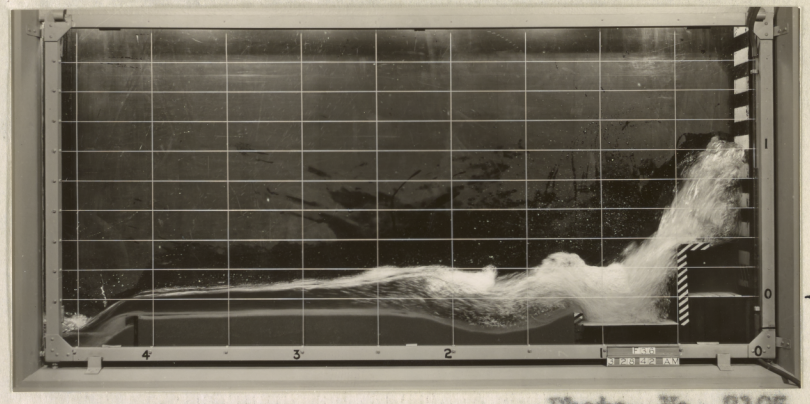

Sluice Opening
d_o = 0.05 ft.

Photo. No. 2105

(b) $F_o = 36$, $h_1 = 6d_o$, $L_1 = 8d_o$, $x_1 = 3d_o$

Discharge continues. Scour-hole develops.

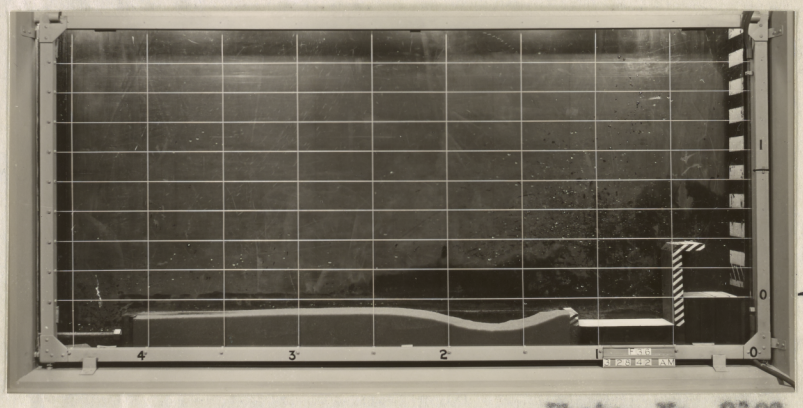

Sluice Opening
d_o = 0.05 ft.

Photo. No. 2106

(c) $F_o = 0$, $h_1 = 6d_o$, $L_1 = 8d_o$, $x_1 = 3d_o$

Scour-hole remaining after sudden stoppage of flow.

FIG. 21.--COMPLETE STRUCTURE OPERATING AT UPPER LIMIT OF TYPE II WITH SAND BED DOWNSTREAM

Static Opening
$q^o = 0.08$ ft.

(a) $E^o = 28'$, $p^f = 64^o$, $i^f = 64^o$, $x^f = 24^o$

Discharge begins. Photo. No. 2108

Static Opening
$q^o = 0.08$ ft.

(b) $E^o = 28'$, $p^f = 64^o$, $i^f = 64^o$, $x^f = 24^o$

Photo. No. 2106

Discharge continues. Scour-hole develops.

Static Opening
$q^o = 0.08$ ft.

(c) $E^o = 0'$, $p^f = 64^o$, $i^f = 64^o$, $x^f = 24^o$

Photo. No. 2108

Scour-hole remaining after sudden stoppage of flow.

FIG. 21.--COMPLETE STRUCTURE OPERATING AT APEX FLOAT OF TYPE II
WITH SAND AND DOWNSTREAM

It is also worthwhile to mention another regime of flow which can occur when the structure is not designed by means of the previously recommended equations 6, 7 and 8. If the biff-wall height or the cap length is less than the value obtained by using the above equations, a regime of flow will occur which has some of the characteristics of Type I flow. This new regime of flow will be known as Type Ia. Type Ia is similar to Type I flow in the respect that, in each case, the not flow has its direction of flow reversed without direct contact with the head wall.

In Type Ia flow, the jet issuing from the sluice opening is not completely turned back on itself either because of incomplete entrance due to the lowness of the wall or because of incomplete turning due to the shortness of the cap. In both cases the diffused jet leaves the edge of the cap with a motion which has a vertical component as well as an upstream (or even downstream) horizontal component. Consequently, less head is required in Type Ia to accomplish the reversal of flow necessary for the stream to discharge over the biff-wall and into the stilling pool than in Type I.

For the condition in which the structure has sufficient cap length and very nearly sufficient biff-wall height, Type Ia flow will occur at low and at average values of F_o, say up to $F_o = 50$; at higher values of F_o, say to $F_o = 100$, Type II flow will be obtained (see Fig. 22). Between the values of the Froude Number at which Types Ia and II are steady, respectively, the flow will oscillate from one pattern to the other. For extremely low walls, the fraction of the high velocity jet which strikes the biff-wall and is turned back by cap is so small that the appearance of the overflow is similar to that produced by a straight biff-wall of height $(h_1 + y_1)$, placed at the location, $(L_1 - x_1)$, from the sluice. Examples of Type Ia flow which are produced by structures with biff-walls of insufficient height are shown as Figs. 23 and 24.

There is also the condition to consider in which the biff-wall is of sufficient height but has inadequate cap overhang. For a structure in which L_1 is small and x_1 short, Type Ia flow will occur up to a certain value of the Froude Number (usually quite high), whereupon the flow pat-

It is also worthwhile to mention another regime of flow which can occur when the structure is not designed by means of the previously recommended equations 6, 7 and 8. If the bliff-wall height or the cap length is less than the value obtained by using the above equations, a regime of flow will occur which has some of the characteristics of Type I flow. This new regime of flow will be known as Type Ia. Type Ia is similar to Type I flow in the respect that, in each case, the nat flow has its direction of flow reversed without direct contact with the head wall.

In Type Ia flow, the jet issuing from the sluice opening is not completely turned back on itself either because of incomplete entrance due to the lowness of the wall or because of incomplete turning due to the shortness of the cap. In both cases the diffused jet leaves the edge of the cap with a motion which has a vertical component as well as an upstream (or even downstream) horizontal component. Consequently, less head is required in Type Ia to accomplish the reversal of flow necessary for the stream to discharge over the bliff-wall and into the stilling pool than in Type I.

For the condition in which the structure has sufficient cap length and very nearly sufficient bliff-wall height, Type Ia flow will occur at low and at average values of F^o, say up to $F^o = 80$; at higher values of F^o, say to $F^o = 100$, Type II flow will be obtained (see Fig. 22). Between the values of the Froude Number at which Types Ia and II are already respectively, the flow will oscillate from one pattern to the other. For extremely low walls, the fraction of the high velocity jet which strikes the bliff-wall and is turned back by cap is so small that the appearance of the overflow is similar to that produced by a straight bliff-wall of height $(p^f + y^f)$, placed at the location, $(L^f - x^f)$, from the sluice. Examples of Type Ia flow which are produced by structures with bliff-walls of insufficient height are shown as Figs. 23 and 24.

There is also the condition to consider in which the bliff-wall is of sufficient height but has inadequate cap overhang. For a structure in which L^f is small and x^f short, Type Ia flow will occur up to a certain value of the Froude Number (usually quite high), whereupon the flow pat-

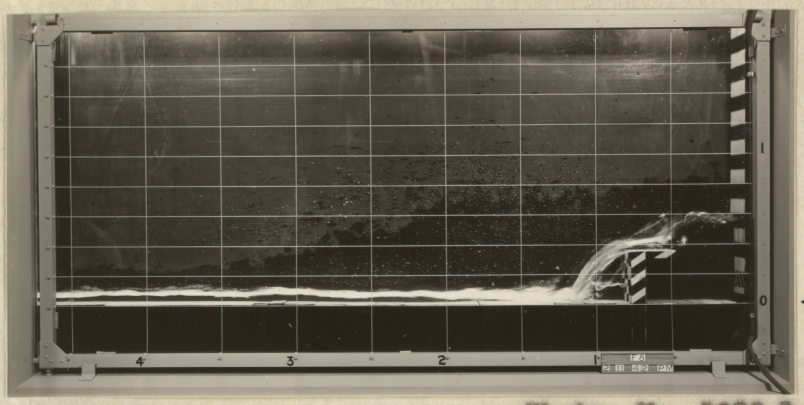

Sluice Opening
d_o = 0.05 ft.

Photo. No. 1960-1

(a) Type Ia Flow - Low Velocity

$F_o = 8$, $h_1 = 6d_o$, $L_1 = 13d_o$, $x_1 = 4d_o$

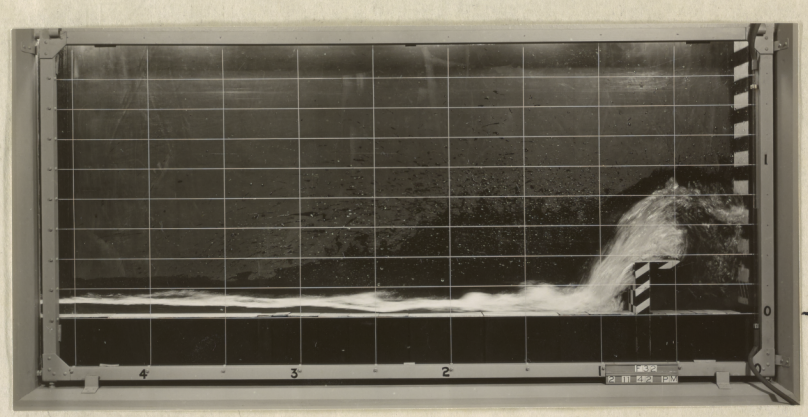

Sluice Opening
d_o = 0.05 ft.

Photo. No. 1960-3

(b) Type Ia Flow - Average Velocity

$F_o = 32$, $h_1 = 6d_o$, $L_1 = 13d_o$, $x_1 = 4d_o$

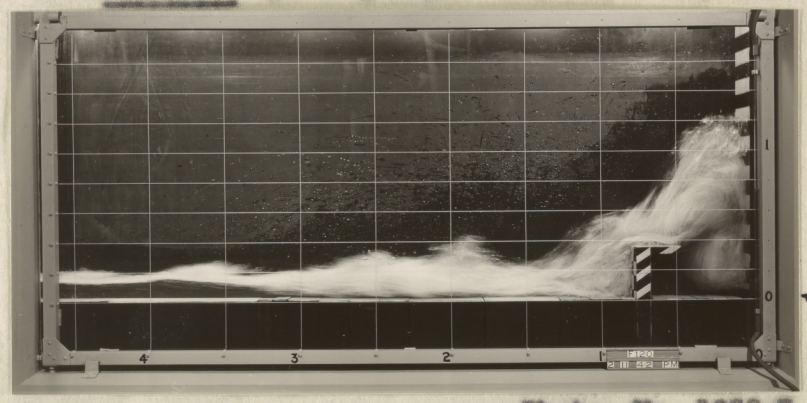

Sluice Opening
d_o = 0.05 ft.

Photo. No. 1960-5

(c) Type II Flow - High Velocity

$F_o = 120$, $h_1 = 6d_o$, $L_1 = 13d_o$, $x_1 = 4d_o$

At high value F_o, flow pattern changes from Ia to II.

FIG. 22.--CONDITION OF INSUFFICIENT BIFF-WALL HEIGHT
In Above Photographs, F_o only is Varied.

Slugs Opening
$q^o = 0.08$ lb.

(a) Type Ia Flow - Low Velocity

$R^o = 8°$, $\beta^1 = 64^o$, $i^1 = 136^o$, $\kappa^1 = 44^o$

Photo. No. 1860-1

Slugs Opening
$q^o = 0.08$ lb.

(b) Type Ia Flow - Average Velocity

$R^o = 32°$, $\beta^1 = 64^o$, $i^1 = 136^o$, $\kappa^1 = 44^o$

Photo. No. 1860-2

Slugs Opening
$q^o = 0.08$ lb.

(c) Type II Flow - High Velocity

$R^o = 120°$, $\beta^1 = 64^o$, $i^1 = 136^o$, $\kappa^1 = 44^o$

Photo. No. 1860-3

At high value R^o, flow pattern changes from Ia to II.

FIG. 22.--CONDITION OF INSTABILITY SLIP-NAIL REGION

In Above Photographs, R^o only is Varied.

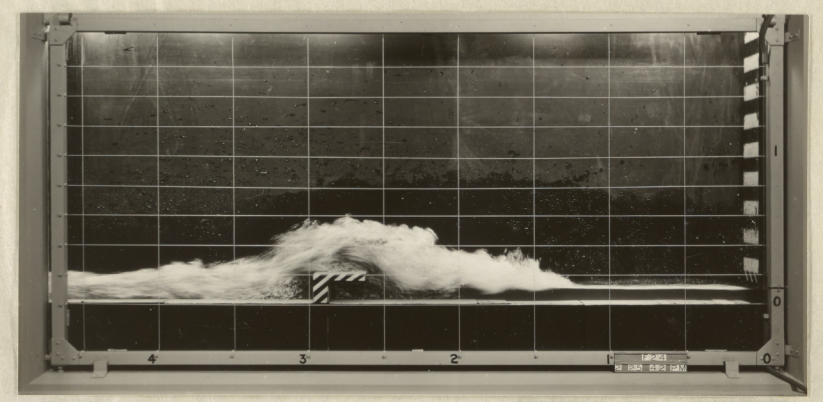

Photo. No. 1962-2

(a)

$F_o = 24$, $d_o = 0.10$ ft.; $h_1 = 1.5d_o$; $h_1 + y_1 = 2d_o$;
$L_1 = 28.5d_o$, $x_1 = 2.5d_o$. Compare with Figure 12a.

This example of Type Ia Flow approaches Condition C (straight biff-wall flow)

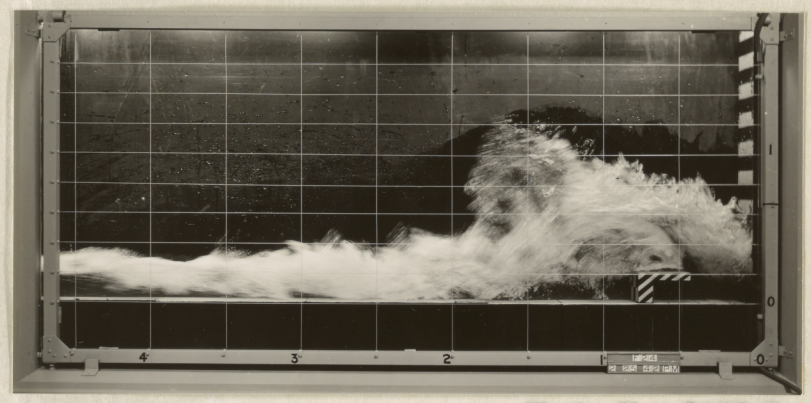

Photo No. 1963-3

(b)

$F_o = 24$, $d_o = 0.10$ ft.; $h_1 = 1.5d_o$, $h_1 + y_1 = 2d_o$;
$L_1 = 6.5d_o$, $x_1 = 2.5d_o$; $L_1 - x_1 = 4d_o$.

Compare with Figure 3c.

FIG. 23.--TYPE Ia FLOW

Very low capped walls do not admit the flow sufficiently to turn it back on itself. Note flow in both cases similar to that obtained using uncapped walls.

Photo. No. 1982-S

(a)

$P^{\circ} = 24^{\circ}$, $q^{\circ} = 0.10$ ft.; $\beta^{J} = 1.84^{\circ}$; $\beta^{J} + \gamma^{J} = 24^{\circ}$;

$I^{J} = 28.84^{\circ}$, $x^{J} = 2.84^{\circ}$. Compare with Figure 12a.

This example of Type Ia Flow approaches Condition c
(straight split-wall flow)

Photo No. 1982-S

(b)

$P^{\circ} = 24^{\circ}$, $q^{\circ} = 0.10$ ft.; $\beta^{J} = 1.84^{\circ}$, $\beta^{J} + \gamma^{J} = 24^{\circ}$;

$I^{J} = 0.84^{\circ}$, $x^{J} = 2.84^{\circ}$; $I^{J} - x^{J} = 44^{\circ}$.

Compare with Figure 3c.

FIG. 28.--TYPE Ia FLOW

Very low capped walls do not admit the flow auxili-
ariy to turn it back on itself. Note flow in both
cases similar to that obtained using unsapped walls.

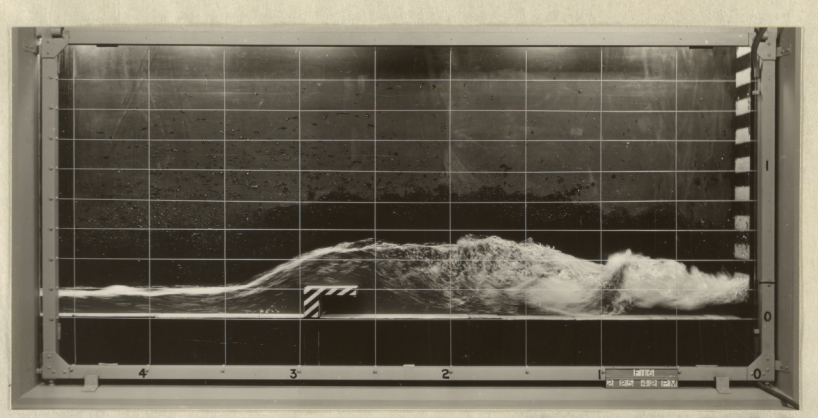

Photo. No. 1962-1

(c)

$F_o = 16$, $d_o = 0.10$ ft.; $h_1 = 1.5d_o$, $h_1 + y_1 = 2d_o$; $L_1 = 28.5d_o$, $x_1 = 2d_o$

Compare with Figures 11a and 23a.

Type Ia flow approaches Condition A -long, which in turn approaches Condition B.

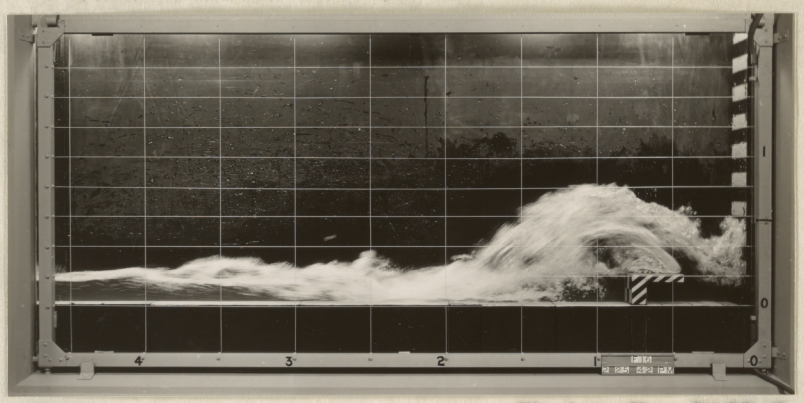

Photo. No. 1963-2

(d)

$F_o = 16$, $d_o = 0.10$ ft.; $h_1 = 1.5d_o$, $h_1 + y_1 = 2d_o$; $L_1 = 6.5d_o$, $x_1 = 2.5d_o$

Compare with Figure 23b

Type Ia approaches Condition A -short.

FIG. 23.--(cont.) - TYPE Ia FLOW

Photo. No. 1962-1

(a) $R^0 = 18,\ d^0 = 0.10$ ft.; $\beta^1 = 1.84^0,\ \beta^1 + \gamma^1 = 24^0;$
$i^1 = 28.84^0,\ x^1 = 24^0$

Compare with Figures 11a and 23a.

Type Ia flow approaches Condition A -long, while in turn approaches Condition B.

Photo. No. 1962-2

(a) $R^0 = 18,\ d^0 = 0.10$ ft.; $\beta^1 = 1.84^0,\ \beta^1 + \gamma^1 = 24^0;$
$i^1 = 6.84^0,\ x^1 = 2.84^0$

Compare with Figure 23b

Type Ia approaches Condition A -short.

FIG. 23.--(cont.) - TYPE Ia FLOW

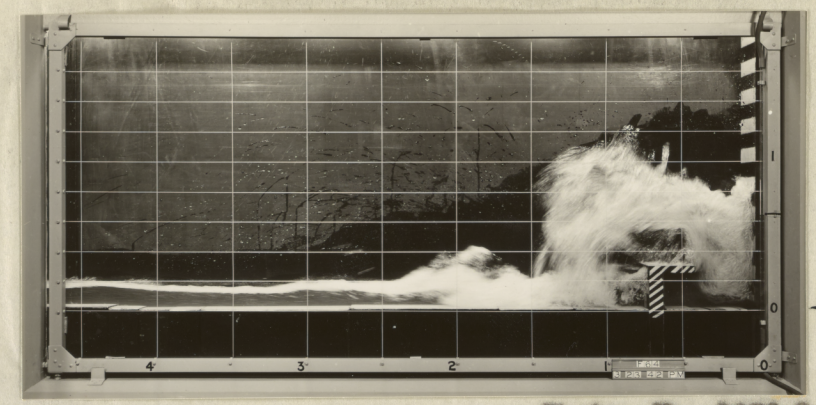

Sluice Opening
d_o = 0.05 ft.

Photo. No. 1976-2

(a)

Type Ia Flow - Wall Height Insufficient
$F_o = 64$, $h_1 = 5d_o$; $L_1 = 12d_o$, $x_1 = 4d_o$

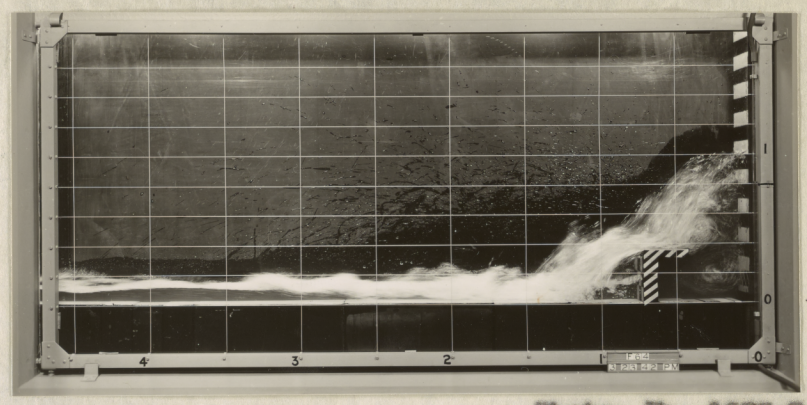

Sluice Opening
d_o = 0.05 ft.

Photo. No. 1977-3

(b)

Type II Flow - Flow Unsteady
$F_o = 64$, $h_1 = 6d_o$; $L_1 = 12d_o$, $x_1 = 4d_o$
Minimum wall height at which Type II flow will occur

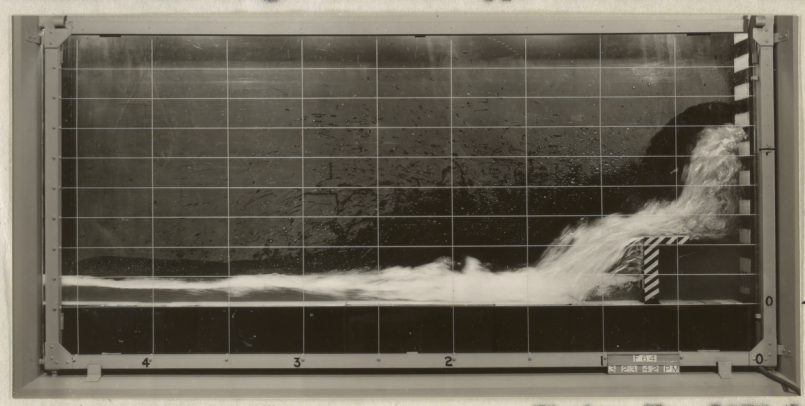

Sluice Opening
d_o = 0.05 ft.

Photo. No. 1979-1

(c)

Type II Flow - Recommended Performance
$F_o = 64$, $h_1 = 8d_o$; $L_1 = 12d_o$, $x_1 = 4d_o$
Structure designed for F = 110. The discharge at F = 64 is 76 percent of the design rate of flow.

FIG. 24.--EFFECT OF WALL HEIGHT ON FLOW TYPE

(a) Photo. No. 1978-2

Type Ia Flow - Well Height Insufficient

$\underline{P^o = 64^o, h^J = 84^o; L^J = 154^o, x^J = 44^o}$

(b) Photo. No. 1977-3

Type II Flow - Flow Uncertain

$\underline{P^o = 64^o, h^J = 84^o; L^J = 154^o, x^J = 44^o}$

Minimum well height at which Type II flow will occur

(c) Photo. No. 1978-1

Type II Flow - Recommended Performance

$\underline{P^o = 64^o, h^J = 84^o; L^J = 154^o, x^J = 44^o}$

Structure designed for P = 110. The discharge at P = 64 is 76 percent of the design rate of flow.

FIG. 54.—METHOD OF RAIL HEIGHT ON FLOW TYPE

tern will suddenly change to Type III. The value of the Froude Number at which the shift from Type Ia to Type III flow occurs depends upon the cap length. For the structure

$h_1 = 5d_o$, $L_1 = 9d_o$; when $x_1 = d_o$, F_o = approx. 120 ;
when $x_1 = 2d_o$, F_o = approx. 90 .

This phenomenon may be analyzed as follows: The jet issuing from the sluice opening flows along the bottom of the baffle chamber and diffuses with the overlying water until it strikes the biff-wall. At this point the direction of the flow is changed through 90° so that the motion of the jet is vertical. Diffusion also takes place as the jet travels through the distance h_1. When the jet reaches the top of the wall and strikes the underside of the cap of overhang length less than the diffused thickness of the jet, the jet will not be turned completely to the horizontal upstream direction. The shorter the cap overhang, the more nearly vertical will be the direction of the jet at the upstream edge of the cap. The relation of the cap overhang to the thickness of the diffused jet determines the angle at which the flow will leave the chamber, for all rates of flow because the thickness of the diffused jet is determined only by the size and shape of the structure.

At low rates of flow, i.e. low values of F_o, turning angles of less than 90° (produced by short caps) will give Type Ia performance. At higher rates of flow, the same angles of turning will still be produced but Type III performance will be obtained. The change will take place when the freely turning overflow has become so large as to strike the head wall before being turned downstream. Obviously, as has previously been pointed out, the change from Type Ia to III flow will take place at lower values of F_o for <u>large</u> cap overhangs and turning angles than for <u>small</u> overhangs and angles. The performance of structures with short caps is shown in Fig. 25.

For the above reasons it was found advisable to use a cap of relatively long overhang so that the length of the cap is always longer than the diffused thickness of the jet. Photographs of cap length study are shown as Fig. 26. The performance will then be that as described earlier in this report, having Type I flow for low Froude Numbers, Type II for intermediate values and Type III for high values of the Froude Number.

this report, having Type I flow for low Froude Numbers, Type II for intermediate values and Type III for high values of the Froude Number.

For the above reasons it was found advisable to use a cap of relatively long overhang so that the length of the cap is always longer than the diffused thickness of the jet. Photographs of cap length study are shown as Fig. 26. The performance will then be that as described earlier in this report, having Type I flow for low Froude Numbers, Type II for intermediate values and Type III for high values of the Froude Number.

- 41 -

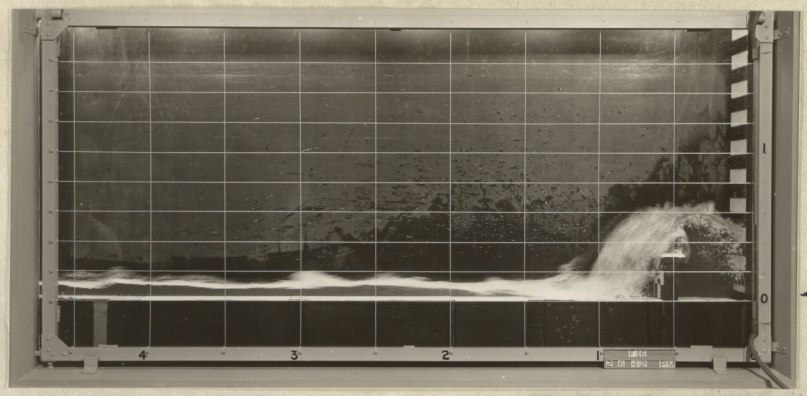

Sluice Opening
d_o = 0.05 ft.

Photo. No. 1950-5

(a)

Type Ia Flow

$F_o = 16$, $h_1 = 5d_o$, $L_1 = 9d_o$, $x_1 = d_o$

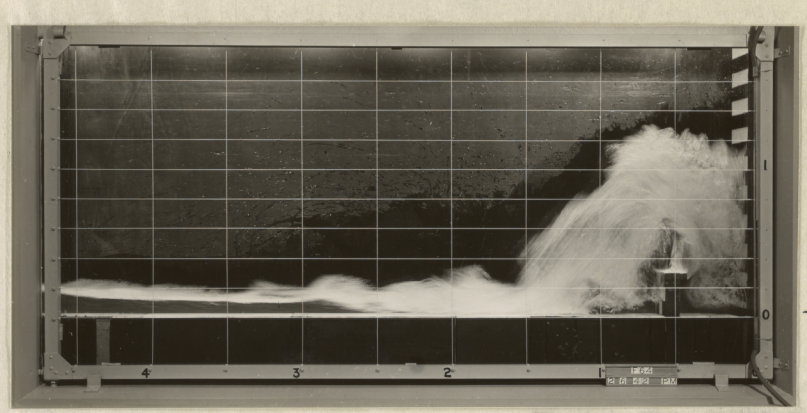

Sluice Opening
d_o = 0.05 ft.

Photo. No. 1950-5

(b)

Type Ia Flow

$F_o = 64$, $h_1 = 5d_o$, $L_1 = 9d_o$, $x_1 = d_o$

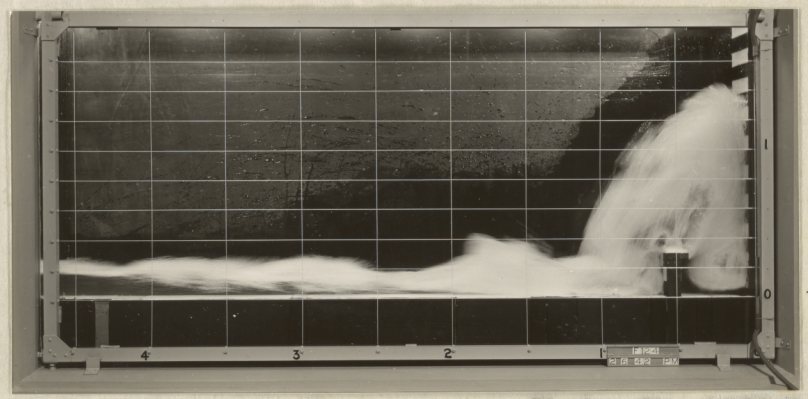

Sluice Opening
d_o = 0.05 ft.

Photo. No. 1950-6

(c)

Type III Flow

$F_o = 124$, $h_1 = 5d_o$, $L_1 = 9d_o$, $x_1 = d_o$

FIG. 25.--BIFF WALLS WITH SHORT CAPS

Note: As Froude Number increases, Type Ia shifts to Type III flow.

(a) Photo. No. 1580-5

Type Ia Flow

$\underline{\beta^0 = 18°,\ \beta^1 = 64^0,\ \Gamma^1 = 94^0,\ x^1 = q^0}$

Sluice Opening
$q^0 = 0.08$ ft.

(b) Photo. No. 1580-8

Type Ia Flow

$\underline{\beta^0 = 66°,\ \beta^1 = 84^0,\ \Gamma^1 = 94^0,\ x^1 = q^0}$

Sluice Opening
$q^0 = 0.08$ ft.

(c) Photo. No. 1580-6

Type III Flow

$\underline{\beta^0 = 124°,\ \beta^1 = 84^0,\ \Gamma^1 = 94^0,\ x^1 = q^0}$

Sluice Opening
$q^0 = 0.08$ ft.

FIG. 25.--SILT WALLS WITH SHORT CAPS

Note: As Froude Number increases, Type Ia shifts to Type III flow.

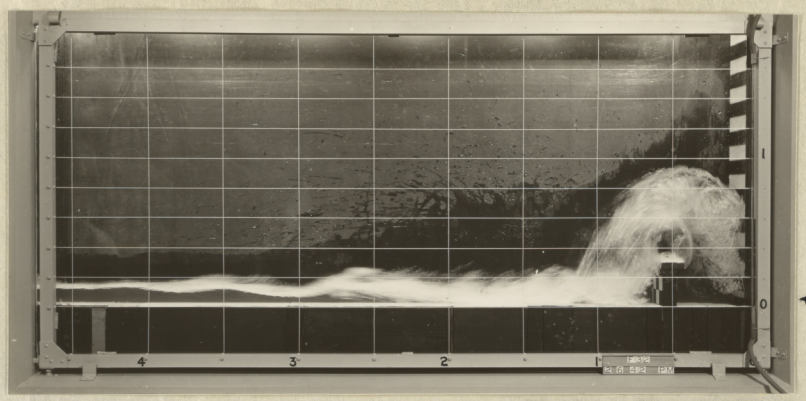

Sluice Opening
d_o = 0.05 ft.

(a) Photo. No. 1950-4

Type Ia Flow - Cap Short

$F_o = 32$; $h_1 = 5d_o$; $L_1 = 9d_o$, $x_1 = d_o$

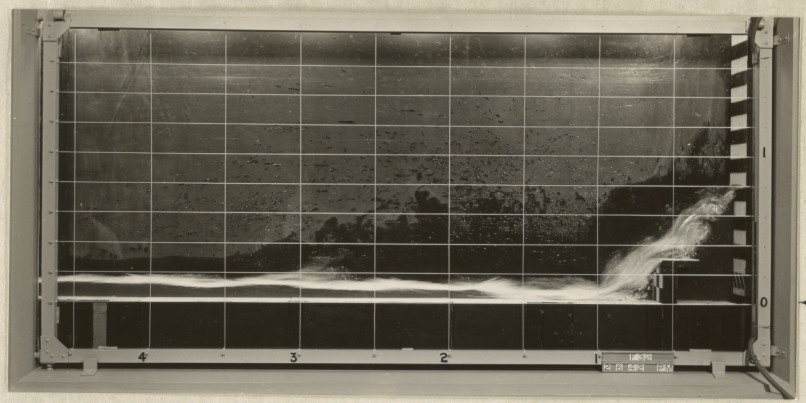

Sluice Opening
d_o = 0.05 ft.

(b) Photo. No. 1952-4

Type II Flow - Good Performance

$F_o = 32$, $h_1 = 5d_o$; $L_1 = 9d_o$, $x_1 = 3d_o$

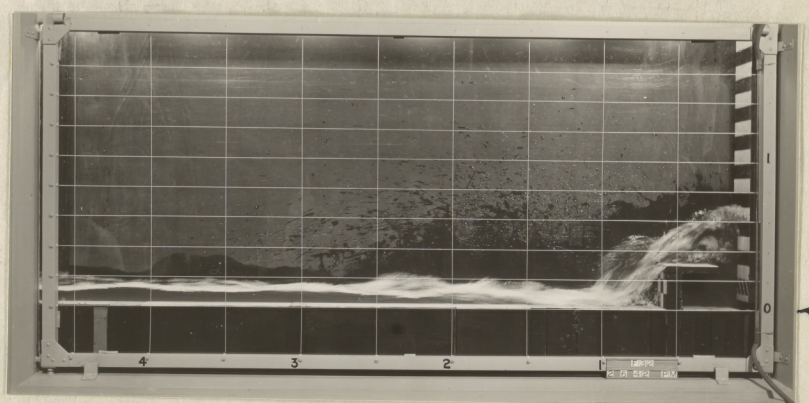

Sluice Opening
d_o = 0.05 ft.

(c) Photo. No. 1954-4

Type II Flow.

Additional cap length does not help much. $F_o = 32$; $h_1 = 5d_o$, $L_1 = 9d_o$; $x_1 = 5d_o$.

FIG. 26.--EFFECT OF CAP LENGTH ON FLOW PATTERN

Flow somewhat unsteady for all cases because wall height, $h_1 = 5d_o$, instead of recommended $h_1 = 6.5d_o$

(a) Photo. No. 1360-4

Type Ia Flow - Crap Short

$P^o = 32$; $h^1 = 32^o$; $l^1 = 96^o$; $x^1 = d^o$

(b) Photo. No. 1362-4

Type IX Flow - Good Performance

$P^o = 32$, $h^1 = 64^o$; $l^1 = 96^o$; $x^1 = 64^o$

(c) Photo. No. 1364-4

Type II Flow.

Additional cap length does not help much. $P^o = 32$; $h^1 = 64^o$, $l^1 = 96^o$; $x^1 = 64^o$.

FIG. 24.—EFFECT OF CAP LENGTH ON FLOW PATTERN

Flow somewhat unsteady for all cases because wall height, $h^1 = 64^o$, instead of recommended $h^1 = 6.64^o$

CAPPED BIFF-WALLS WITH DROPPED FLOORS

Since jet diffusion is a major factor in energy dissipation in even the shortest biff-wall structures, it occurred to the writers that additional opportunity for jet diffusion might increase energy dissipation. Tests were made with this opportunity provided by dropping the biff-wall chamber-floor as much as $p_o = 2d_o$. (see Fig. 14).

The results of these tests indicated that dropped floors may be desirable when F_o is greater than 32 because they reduce the energy remaining in the stream and thus the height of rise over the biff-wall chamber. At lower values of F_o this reduction is quite small compared with the depth of overflow over the biff-wall and thus not of much worth. To secure the advantages of dropped floors, slight increases in biff-wall height are necessary. From the few observations made, the following formula is suggested:

$$h_1 = 2d_o + \frac{1}{2} \cdot L_1 + 0.007 \left(\frac{L_1}{d_o}\right)^2 \cdot p_o \qquad (10)$$

or

$$\frac{h_1}{d_o} = 2 + \frac{1}{2} \cdot \frac{L_1}{d_o} + 0.007 \left(\frac{L_1}{d_o}\right)^2 \cdot \frac{p_o}{d_o}$$

Use of this formula should be restricted to values of L_1 between $8d_o$ and $12d_o$, unless more tests prove it to be extensible.

Figures 27, 28, and 29 show that dropping the floor $p_o = d_o$ is desirable at high values of F_o, and that the drop of $p_o = 2d_o$ may be justified in some cases.

CAPPED SILT-WALLS WITH DROPPED FLOORS

Since jet diffusion is a major factor in energy dissipation in cavan the shortest silt-wall structures, it occurred to the writers that additional opportunity for jet diffusion might increase energy dissipation. Tests were made with this opportunity provided by dropping the silt-wall chamber-floor as much as $D^o = 2d^o$, (see Fig. 14).

The results of these tests indicated that dropped floors may be desirable when F^o is greater than 22 because they reduce the energy remaining in the stream and thus the height of rise over the silt-wall chamber. At lower values of F^o this reduction is quite small compared with the depth of overflow over the silt-wall and thus not of much worth. To secure the advantages of dropped floors, slight increases in silt-wall height are necessary. From the few observations made, the following formula is suggested:

$$\frac{d_1}{d^o} = 2 + \frac{2}{3}\frac{d^o}{I^J} + 0.004\left(\frac{d^o}{I^J}\right)^2 \cdot \frac{D^o}{d^o} \qquad (10)$$

or

$$I^J = 2d^o + \frac{2}{3}I^J + 0.004\left(\frac{d^o}{I^J}\right)^2 \cdot D^o$$

Use of this formula should be restricted to values of I^J between $8d^o$ and $12d^o$, unless more tests prove it to be extensible.

Figures 27, 28, and 29 show that dropping the floor $D^o = d^o$ in desirable at high values of F^o, and that the drop of $D^o = 2d^o$ may be justified in some cases.

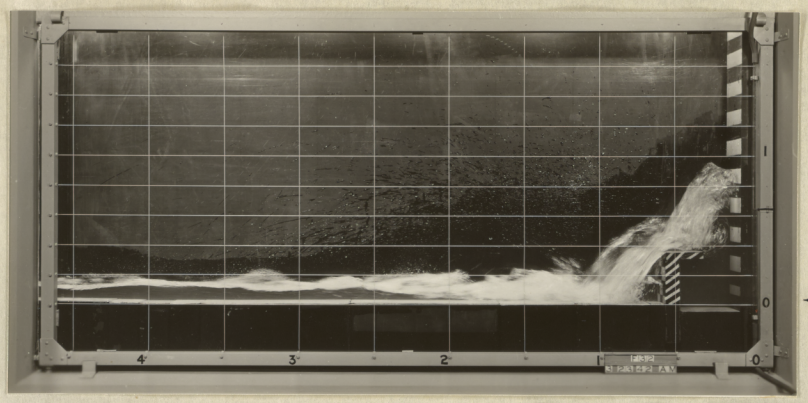

Back-Pressure Indication Not Reliable

Sluice Opening d_o = 0.05 ft.

(a) Photo. No. 1973-2

Type II

$F_o = 32$, $h_1 = 6d_o$; $L_1 = 8d_o$, $x_1 = 3d_o$, $p_o = d_o$

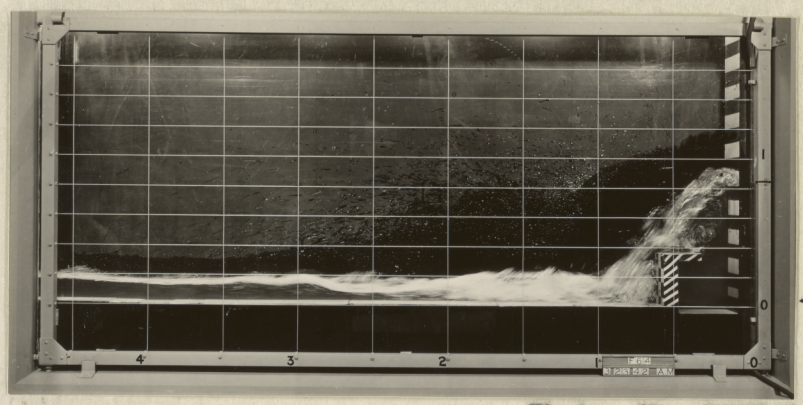

Sluice Opening d_o = 0.05 ft.

(b) Photo. No. 1973-3

Type II

$F_o = 64$, $h_1 = 6d_o$, $L_1 = 8d_o$, $x_1 = 3d_o$, $p_o = d_o$

Compare with Figure 20b

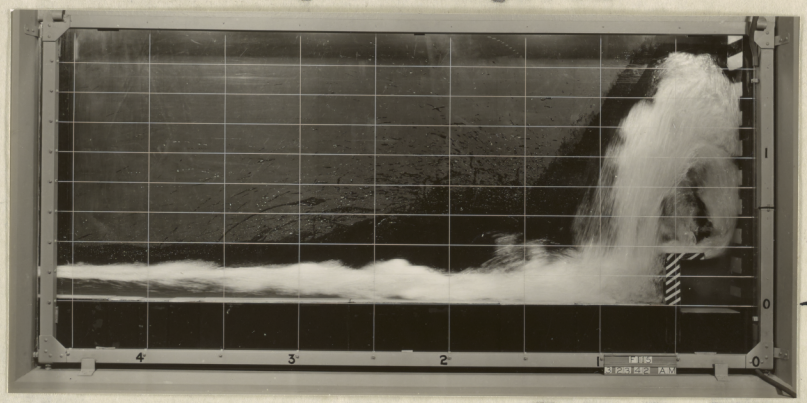

Back-Pressure Indication Not Reliable

Sluice Opening d_o = 0.05 ft.

(c) Photo. No. 1973-4

Type III

$F_o = 115$, $h_1 = 6d_o$, $L_1 = 8d_o$, $x_1 = 3d_o$, $p_o = d_o$

FIG. 27.--EFFECT OF DROPPED FLOOR ON PERFORMANCE OF STRUCTURE

Floor dropped by the amount $p_o = d_o$

(a) Photo. No. 1972-5

Type II

$P^o = 82°$, $p^1 = 64^o$; $T^1 = 84^o$, $x^1 = 34^o$, $P^o = q^o$

(β) Photo. No. 1972-3

Type II

$P^o = 84°$, $p^1 = 64^o$, $T^1 = 84^o$, $x^1 = 34^o$, $P^o = q^o$

Compare with Figure 20b

(c) Photo. No. 1972-4

Type III

$P^o = 116°$, $p^1 = 64^o$, $T^1 = 84^o$, $x^1 = 34^o$, $P^o = q^o$

FIG. 21.--EFFECT OF DROPPED FLOOR ON PERFORMANCE OF STRUCTURES

Floor dropped by the amount $P^o = q^o$

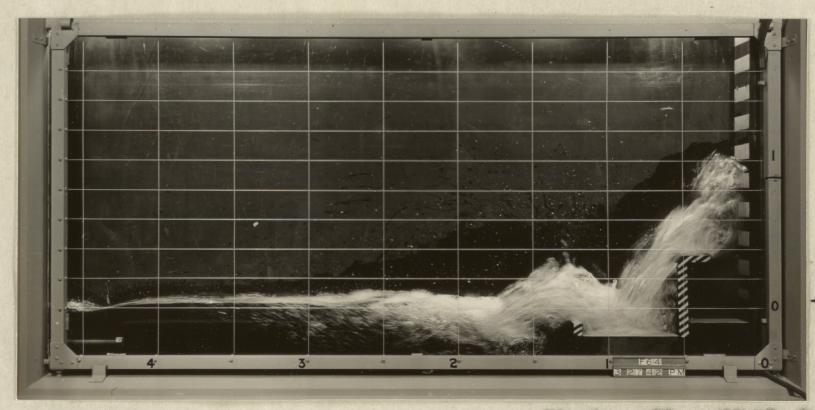

Sluice Opening
d_o = 0.05 ft.

Photo. No. 2101-2

(a)

Type II Flow - Good Performance
$F_o = 64$, $h_1 = 6d_o$, $L_1 = 8d_o$, $x_1 = 3d_o$; $\underline{p_o = 2d_o}$

Compare with Figures 27b and 20b. Conditions identical except for dropped floor, - $p_o = 2d_o$.
Note improved performance.

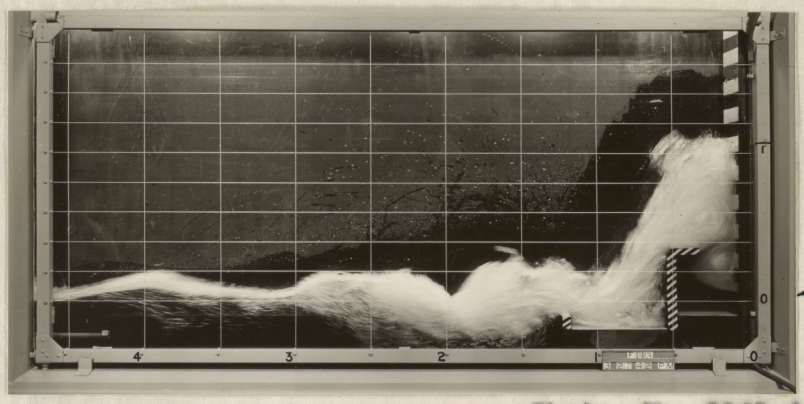

Sluice Opening
d_o = 0.05 ft.

Photo. No. 2101-4

(b)

Type III → II, - Structure Somewhat Overloaded
$F_o = 113$, $h_1 = 6d_o$, $L_1 = 8d_o$, $x_1 = 3d_o$, $\underline{p_o = 2d_o}$

Compare with Figures 27c and 19b. Note greatly improved performance gained by dropping floor.

FIG. 28.---EFFECT OF DROPPED FLOOR ON PERFORMANCE OF STRUCTURE

Shown above are two identical structures with the discharge varied. (a) $F_o = 64$, (b) $F_o = 113$.
Floor dropped by the amount, $p_o = 2d_o$.

Photo. No. 2103-5

(a)

Type II Flow - Good Performance

$P_1^o = 64^o$, $P_2^o = 64^o$, $I_1^o = 84^o$, $x_1^o = 54^o$; $\underline{P_3^o = 24^o}$

Compare with Figures 17b and 20b. Conditions identical except for dropped floor, $P_3^o = 24^o$.
Note improved performance.

Sluice Opening
$d_1^o = 0.08$ ft.

Photo. No. 2103-6

(b)

Type III → II - Structure Somewhat Overloaded

$P_1^o = 112$, $P_2^o = 64^o$, $I_1^o = 84^o$, $x_1^o = 54^o$, $\underline{P_3^o = 24^o}$

Compare with Figures 17c and 19b. Note greatly improved performance gained by dropping floor.

Sluice Opening
$d_1^o = 0.08$ ft.

FIG. 18.---EFFECT OF DROPPED FLOOR ON PERFORMANCE OF STRUCTURE

Floor dropped by the amount, $P_3^o = 24^o$.

Curves above are two identical structures with the discharge varied. (a) $P_1^o = 64^o$, (b) $P_1^o = 112$.

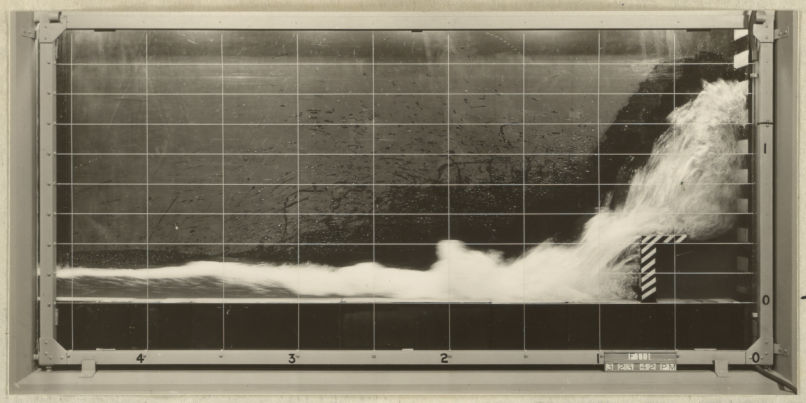

Sluice Opening
d_o = 0.05 ft.

(a) Photo. No. 1979-2

Type II Flow - Good Performance.

$F_o = 111$, $h_1 = 8d_o$, $L_1 = 12d_o$, $x_1 = 4d_o$, $p_o = 0$

Compare with Figure 18c. Instantaneous photographs indicate normal variations in flow.

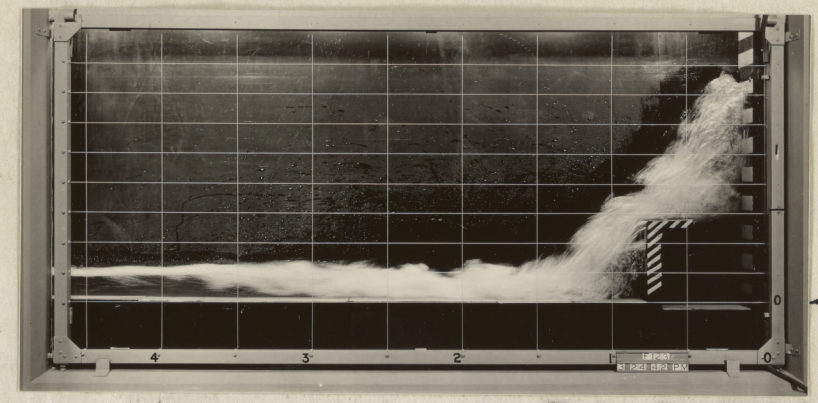

Back Pressure Indication Not Reliable

Sluice Opening
d_o = 0.05 ft.

(b) Photo. No. 1991-2

Type II Flow - Better Performance

$F_o = 123$, $h_1 = 10d_o$, $L_1 = 12d_o$, $x_1 = 4d_o$; $p_o = d_o$

Steadier flow and reduced air entrainment were observed.

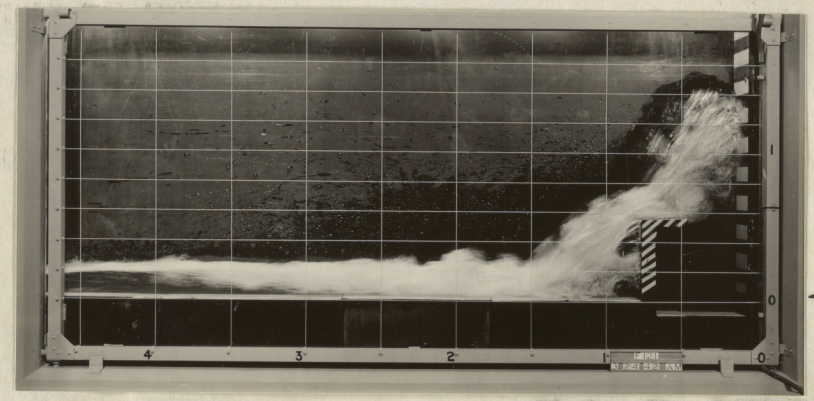

Back Pressure Indication Not Reliable

Sluice Opening
d_o = 0.05 ft.

(c) Photo. No. 1986-2

Type II Flow - Best Performance

$F_o = 121$, $h_1 = 10d_o$, $L_1 = 12d_o$, $x_1 = 4d_o$, $p_o = 2d_o$

FIG. 29.---EFFECT OF DROP FLOOR FOR LARGER STRUCTURES

Note increase in wall height required when floor dropped. Dropping floor does not appear to improve performance as much for large as for small structures.

(a) Photo. No. 1878-S

Type II Flow - Good Performance.

F^o = 111°, h^1 = 64°, L^1 = 124°, x^1 = 44°, P^o = 0

Compare with Figure 18c. Instantaneous photo-graphs indicate normal variations in flow.

(b) Photo. No. 1881-S

Type II Flow - Better Performance

F^o = 125°, h^1 = 106°, L^1 = 124°, x^1 = 44°, P^o = d^o

Steadier flow and reduced air entrainment were observed.

(c) Photo. No. 1886-S

Type II Flow - Best Performance

F^o = 131°, h^1 = 104°, L^1 = 124°, x^1 = 44°, P^o = $2d^o$

FIG. 20.--METHOD OF DROP FLOOR FOR LARGER EXHAUSTERS

Note increase in wall height required when floor dropped. Dropping floor does not appear to improve performance as much for large as for small structures.

SUMMARY

While the following statements are based on observation of flow in two dimensions they are believed to be applicable to pipe outlet designs as well as sluice outlets.

1. Capped biff-walls of very small heights may be used to dissipate energy from pipe outlets discharging at any velocity.

2. The height of such walls is determined by the pipe diameter and not directly by the velocity of discharge.

3. Long overhanging caps are required for most effective energy dissipation and least size of structure.

4. Capped biff-walls should be placed at a short distance, generally less than twice the wall height, from the pipe outlet.

5. Dropped floors increase the energy dissipation possibilities of biff-wall structures.

6. Rules are available for the proportioning of capped biff-wall structures in two-dimensional applications.

SUMMARY

While the following statements are based on observation of flow in two dimensions they are believed to be applicable to pipe outlet designs as well as sluice outlets.

1. Capped bluff-walls of very small heights may be used to dissipate energy from pipe outlets discharging at any velocity.

2. The height of such walls is determined by the pipe diameter and not directly by the velocity of discharge.

3. Long overhanging caps are required for most effective energy dissipation and least size of structure.

4. Capped bluff-walls should be placed at a short distance, generally less than twice the wall height, from the pipe outlet.

5. Dropped floors increase the energy dissipation possibilities of bluff-wall structures.

6. Rules are available for the proportioning of capped bluff-wall structures in two-dimensional applications.

APPENDIX A

Minimum Biff Wall or Sill Height for the Forced Shock Wave

During the tests of the straight biff-wall structure, it was noted that the flow over the wall in Condition C, the forced shock wave, resembled closely that produced at the end sill of stilling pools. (See Morris and Johnson, Hydraulic Design of Drop Structures for Gully Control, Proc. Am. Soc.C.E., January 1942; also Morris and Jones, Hydraulic Model Tests of Conventional Drop Structures, 1940.)

The drop structure studies produced a new rule for the determination of end-sill heights:

$$p = 0.5d_o \qquad (11)$$

Because this equation is essentially empirical and because stilling pools of the type applied to drop structures may be used below biff-walls, special study was given to the determination of the minimum height of wall or sill for the production of Condition C.

Two series of experiments were conducted: (a) one in which the overflow was produced without submergence by means of a narrow crested biff-wall and a depressed channel, and (b) one in which the overflow was submerged by water standing on the channel floor extending downstream from and level with the crest of the end sill. In each series, tests were made at two distances, L_1, from the sluice opening, at several wall or sill heights, p*, and at many different Froude Numbers. Most of the tests were made at rates of flow near that separating Conditions C and D.

The range of tests was:

d_o	0.05 ft. and 0.10 ft.
p	d_o to $3.6d_o$
L_1	$20d_o$ and $70d_o$
$F_o = \frac{V_o^2}{gd_o}$	10 to 137

---

* The nomenclature of the stilling pool, rather than that of the biff-wall chamber, has been employed.

APPENDIX A

Minimum Sill Wall or Sill Height for the Forced Shock Wave

During the tests of the straight *sill-wall* structure, it was noted that the flow over the *wall* in Condition C, the forced shock wave, resembled closely that produced at the end *sill* of *stilling pools*. (See Morris and Johnson, Hydraulic Design of Drop Structures for Gully Control, Proc. Am. Soc.C.E., January 1942; also Morris and Jones, Hydraulic Model Tests of Conventional Drop Structures, 1940.)

The drop structure studies produced a new rule for the determination of end-sill heights:

$$p = 0.8 d_o \qquad (11)$$

Because this equation is essentially empirical and because *stilling pools* of the type applied to drop structures may be used below *sill-walls*, special study was given to the determination of the minimum height of *wall* or *sill* for the production of Condition C.

Two series of experiments were conducted: (a) one in which the overflow was produced without submergence by means of a narrow crested *sill-wall* and a depressed channel, and (b) one in which the overflow was submerged by water standing on the channel floor extending downstream from and level with the crest of the end *sill*. In each series, tests were made at two distances, l'_1, from the sluice opening, at several *wall* or *sill* heights, p*, and at many different Froude Numbers. Most of the tests were made at rates of flow near that separating Conditions C and D.

The range of tests was:

d_o	0.08 ft. and 0.10 ft.
p	d_o to $5.8 d_o$
l'_1	$20 d_o$ and $70 d_o$
$F_o = \frac{v_o}{\sqrt{g d_o}}$	10 to 15?

---

* The nomenclature of the *stilling pool*, rather than that of the *sill-wall* chapter, has been employed.

The data taken in these tests are plotted on a chart, Figure 30, in which p/d_c is shown as a function of F_o. No distinction was made between measurements at $L_1 = 20d_c$ and those at $70d_c$ in plotting the data. Three bold lines have been drawn in Figure 30. The two curved and inclined lines in the upper left corner of the diagram indicate the locus of points at which the hydraulic jump replaces the forced shock-wave for either the submerged or the unsubmerged tests. These hydraulic jump points were experimentally determined. The third line is drawn horizontally through the field of data at a large enough value of p/d_c to secure positive formation of Condition C at values of F_o greater than 20. The equation of this line

$$p = 0.6d_c \qquad (12)$$

is recommended for the use in calculating minimum biff-wall heights and sill heights for flow from sluice outlets. Comparison of the data of Figure 30 with the results of the drop structure experiments indicates that there is a difference between the sluice outflow condition and that obtained in the stilling pool of the drop structure. The difference may be either in the contracted flow effects or in the unusual velocity distribution produced as the drop structure overfall strikes the apron. The performance shown in Figure 15d of the Morris and Johnson paper or on page 39, photograph 1682-C of the Morris and Jones paper where flow contraction was eliminated entirely at $p/d_c = 0.48$ is evidence pointing toward flow contraction as a principle cause of difference. Therefore, except for extremely wide or uncontracted drop structures, it should not be necessary to replace equation 11 with equation 12.

Some of the points plotted in Figure 30 are shown by the photographs in Figures 4, 5, and 13 in the discussion of straight biff-walls. Also, during the tests described in this appendix, additional information was obtained for plotting in Figures 2 and 7 of the straight biff-wall discussion.

The data taken in these tests are plotted on a chart, Figure 30, in which p/q^0 is shown as a function of P^0. No distinction was made between measurements at $P^1 = 20\%^0$ and those at $70\%^0$ in plotting the data. Three bold lines have been drawn in Figure 30. The two curved and inclined lines in the upper left corner of the diagram indicate the locus of points at which the hydraulic jump replaces the forced shock-wave for either the submerged or the unsubmerged tests. These hydraulic jump points were experimentally determined. The third line is drawn horizontally through the field of data at a large enough value of p/q^0 to secure positive formation of Condition C at values of P^0 greater than 20. The equation of this line

$$p = 0.64^0 \qquad (12)$$

is recommended for the use in calculating minimum bilf-wall heights and sill heights for flow from sluice outlets. Comparison of the data of Figure 30 with the results of the drop structure experiments indicates that there is a difference between the sluice outflow condition and that obtained in the stilling pool of the drop structure. The difference may be either in the contracted flow effects or in the unusual velocity distribution produced as the drop structure overfall strikes the apron. The performance shown in Figure 18d of the Morris and Johnson paper or on page 39, photograph 1822-C of the Morris and Jones paper where flow contraction was eliminated entirely at $p/q^0 = 0.48$ is evidence pointing toward flow contraction as a principle cause of difference. Therefore, except for extremely wide or uncontracted drop structures, it should not be necessary to replace equation 11 with equation 12.

Some of the points plotted in Figure 30 are shown by the photographs in Figures 4, 5, and 12 in the discussion of straight bilf-walls. Also, during the tests described in this appendix, additional information was obtained for plotting in Figures 3 and 7 of the straight bilf-wall discussion.

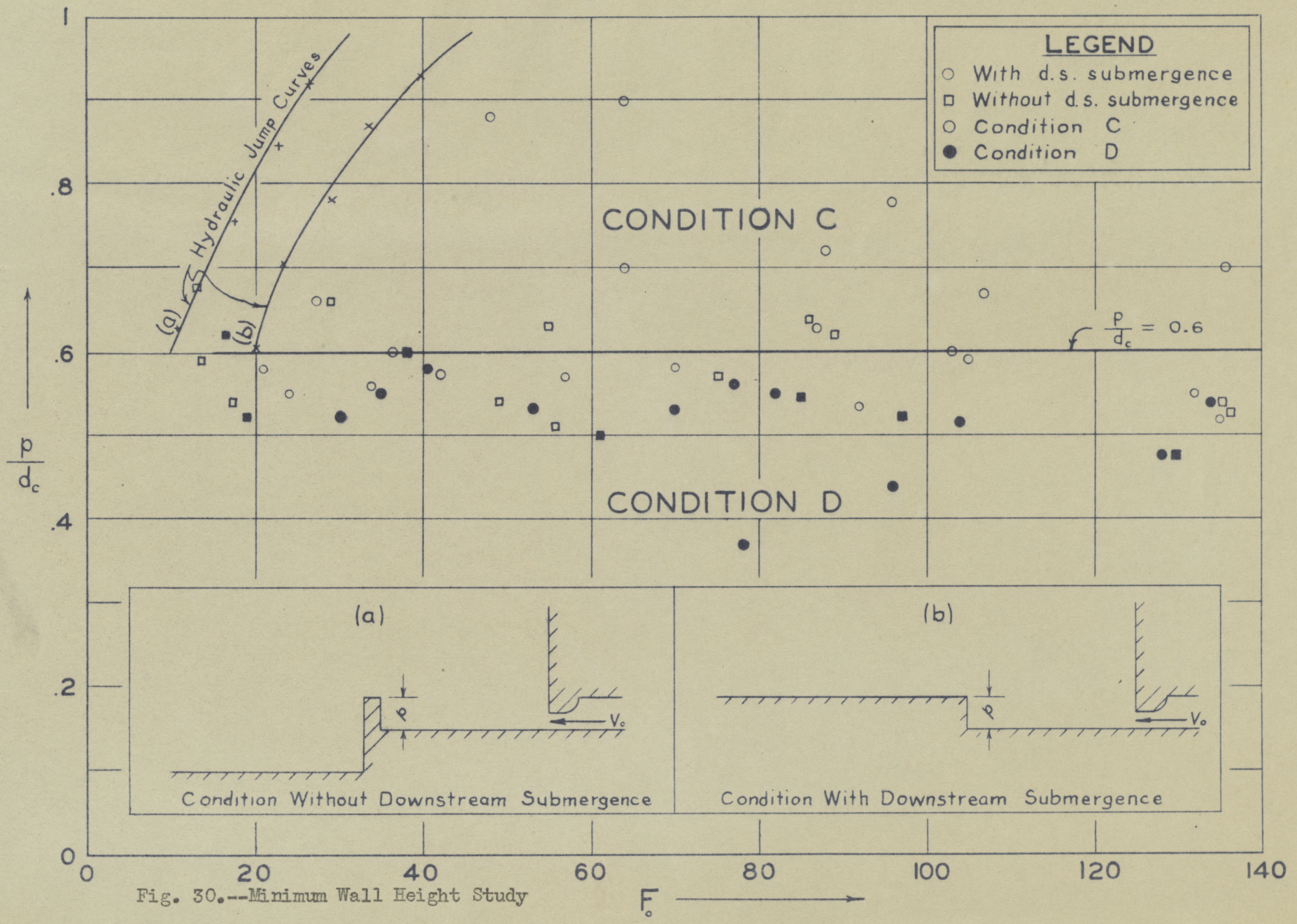

Fig. 30.--Minimum Wall Height Study